



Long-Range Forecasting and Climate Research

METEOROLOGICAL OFFICE

148179

22 JUL 1986

LIBRARY

The climate of the world

II — Forcing and feedback processes

by

C.K. Folland

LONDON, METEOROLOGICAL OFFICE.
Long-range Forecasting and Climate Research ~~Memorandum~~
Memorandum No. LRFC 2.
The climate of the world. II. Forcing and
feedback processes.

LRFC 2

08180786

FH1B

March 1986

ORGS UKMO L

National Meteorological Library
FitzRoy Road, Exeter, Devon. EX1 3PB

FH1B

LONG RANGE FORECASTING AND CLIMATE RESEARCH MEMORANDUM NO. 2
(LRFC 2)

THE CLIMATE OF THE WORLD

II - FORCING AND FEEDBACK PROCESSES

by

C K FOLLAND

BASED ON TWO ADVANCED LECTURES DELIVERED
TO THE SCIENTIFIC OFFICERS' COURSE,
METEOROLOGICAL OFFICE COLLEGE, MARCH 1985

Met O 13 (Synoptic Climatology Branch)
Meteorological Office
London Road
Bracknell
Berkshire RG12 2SZ

March 1986

Note. This paper has not been published. Permission to quote from it should be obtained from the Assistant Director (Synoptic Climatology), Meteorological Office.

This Memorandum is the second in a series of six on:

LONG RANGE FORECASTING AND CLIMATE RESEARCH MEMORANDUM NO. 2
(LRFC 2)

THE CLIMATE OF THE WORLD

BY

C K Folland and D E Parker

C K FOLLAND

BASED ON TWO ADVANCED LECTURES DELIVERED
TO THE SCIENTIFIC OFFICERS' COURSE,
METEOROLOGICAL OFFICE COLLEGE, MARCH 1985

Based on nine Advanced Lectures delivered by C K Folland to the Scientific Officers' Course 1-7 March 1985, and one Advanced Lecture delivered by D J Carson in March 1982.

Met O 13 (Synoptic Climatology Branch)
Meteorological Office
London Road
Bracknell
Berkshire RG2 52E

March 1985

Note: This paper has not been published. Permission to quote from it should be obtained from the Assistant Director (Synoptic Climatology), Meteorological Office.

INDEX TO SERIES

- LRFC 1. INTRODUCTION AND DESCRIPTION OF WORLD CLIMATE.
(Advanced Lectures 1 and 2). C K Folland
- LRFC 2. FORCING AND FEEDBACK PROCESSES.
(Advanced Lectures 3 and 4). C K Folland
- LRFC 3. EL NINO/SOUTHERN OSCILLATION AND THE QUASI-BIENNIAL OSCILLATION.
(Advanced Lecture 5). C K Folland and D E Parker
- LRFC 4. CLIMATIC CHANGE: THE ANCIENT EARTH TO THE 'LITTLE ICE AGE'.
(Advanced Lectures 6 and 7). C K Folland
- LRFC 5. CLIMATIC CHANGE: THE INSTRUMENTAL PERIOD.
(Advanced Lecture 8). C K Folland and D E Parker
- LRFC 6. CARBON DIOXIDE AND CLIMATE (WITH APPENDIX ON SIMPLE CLIMATE MODELS).
(Advanced Lecture 9 plus an Advanced Lecture delivered by D J Carson in March 1982).

ADVANCED LECTURE NO. 3

CLIMATE FORCING AND FEEDBACK PROCESSES I - FORCING FROM ABOVE

PART I - Variations in Solar Radiation and Climate Variability

3.1.1 Earth's climate is in principle sensitive to fluctuations of solar radiation if they persist for sufficient lengths of time. The average flux of energy from the sun at the mean radius of the earth is called the solar constant S and is about:-

$$S = 1370 \pm 15 \text{ Wm}^{-2}$$

Now the average flux of solar radiation received on the earth is, if R is the earth's radius:-

$$E_s = \pi R^2 S$$

The area of the earth's surface is $4\pi R^2$ so the average amount of energy received by the earth-atmosphere system is

$$S/4 = 342 \pm 4 \text{ Wm}^{-2}$$

It is easy to see that if the axis of rotation of the earth was normal to the plane intersecting the sun and all points in the earth's orbit, E_s would vary between a maximum ($S = 436 \text{ Wm}^{-2}$) at the equator to zero at the poles. However the tilt of the earth's rotation axis, from this position is currently 23.44° . This results in large seasonal variations in radiation, though the simple calculation above is quite accurate close to the equator. Fig 3.1a shows the current zonally averaged radiation balance of the earth; the seasonal variations of insolation above the atmosphere are shown in Fig 3.1b. A fraction $A = 0.3$ (approximately) of the radiation is reflected or scattered; this fraction is called the albedo. Figs 3.2 and 3.3 are a good guide to the surface albedo of the world with and without clouds. So the effective temperature of the earth is approximately given by

$$\sigma T_e^4 = (1-A)S/4 \quad (1)$$

Here we have assumed that the emissivity of the earth is one (not quite true), while T_e is approximately the mass-weighted temperature of the atmosphere, subject to some modification by dynamical processes. The sensitivity of T_e to S is shown by differentiating equation (1)

$$4 \sigma T_e^3 \Delta T_e = \frac{\partial T_e}{\partial S} \Delta S + \frac{\partial T_e}{\partial A} \Delta A \quad (2)$$

If a 1% increase in S was accompanied by a 0.01 decrease in A due to the associated melting of snow and ice, or perhaps a reduction in low-cloudiness, we obtain:-

$$\Delta T_e = + 1.5^\circ\text{C}/1\% \text{ increase in } S$$

If $\Delta A = 0$ then ΔT_e is only $+0.6^\circ\text{C}/1\%$ increase in S . So the sensitivity of the climate to S strongly depends on any associated changes in albedo. The ice/snow component of the feedback between solar radiation and climate is often called the ice-albedo feedback but its magnitude is uncertain. Nevertheless the climate system is very sensitive to long-lasting small changes in S .

3.1.2 Change of S

Does S actually change? Astronomers can say little about the fluctuations of S on short time scales but they believe it varies on geological time scales. Current theories suggest that S progressively increases as the sun gets older so that its value was perhaps 30% less 4 thousand million years ago than now. This question will be discussed in lecture 6.

Leaving aside the regular change of nearly 7% in radiation flux between January and July due to the fact that the earth currently moves in an elliptic orbit with eccentricity 0.0167, there are recent measurements of very small changes in S from the Solar Maximum Mission spacecraft. Fig 3.4 (Hudson (1983)) shows rapid variations in S measured by a cavity radiometer at a time of high solar activity (when many sunspots are sometimes visible on the solar disk). Although the mean absolute value of S shown in Fig. 3.4 (1368.2 Wm^{-2}) is in fact only accurate to about $\pm 0.5\%$ ($\pm 7 \text{ Wm}^{-2}$) the relative changes in S are believed to be accurate to $\pm 0.1\%$ (say $\pm 1 \text{ Wm}^{-2}$). The variations in Fig 3.4 approach four times this size and have a typical range of 0.2% over say a 10 day period. These variations have been shown to be due to 'sunspot blocking'; ie if there are many sunspots visible from the earth they block the solar radiation at least temporarily, since sunspots are cooler than the remainder of the surface of the sun (the sunspot temperatures are typically about 4000°C rather than the normal 6000°C , and warmer areas (formulae) sometimes surrounding sunspots do not compensate). Thus the radiation from the very small area covered by sunspots is reduced by a multiplying factor of $(4/6)^4$, about 0.2. These measurements are the first that indicate a real variation in the solar constant, though of course by very small amounts on short time scales. Fig 3.5 shows an imaginative but plausible reconstruction of variations of S over the last century from these observations, past sunspot data and a few other assumptions. The variations in Fig 3.5 seem insufficient or at least to last insufficiently long to have much effect on climate. Solar activity and the number of sunspots vary on several timescales eg 11 years, about 80 years and possibly longer time scales (Eddy (1983)) (Fig 3.6). These variations of solar activity are also associated with fluctuations in the intensity of ultra violet radiation so that ultra violet radiation intensity increases as solar activity increases.

Many authors have in the past associated widespread cooler climates with a lack of sunspots and thus by implication a lower solar constant (eg during the Maunder "minimum" of the seventeenth century shown in Fig 3.6) when sunspots may have been virtually absent. So recent satellite measurements of S paradoxically only confuse ideas about the relationship between sunspots, variations in the solar constant and climate variations (see Lecture 8). Gilliland (1983) has claimed to detect small changes in solar radius on a dominant time scale of 76 years using measurements of

uncertain homogeneity made by astronomers since the mid-nineteenth century. He tentatively associates a larger radius with an enhanced solar radiation flux etc. Unfortunately this kind of evidence has to be seriously considered until the time comes when accurate measurements of the solar constant made over many years are available. Fortunately such measurements are still being made by satellites.

3.1.3 Changes in the distribution of solar radiation on earth with the seasons

Changes in the seasonal distribution of radiation occur on long time scales due to fluctuations in the orbit of the earth. Assuming no intrinsic change in S , the changes in orbit are accompanied by very small apparent changes in S because the mean earth-sun distance changes only by small amounts. However seasonal values of radiation received at given latitudes on earth change much more. The fact that the earth's orbit has varied in a systematic way in the past was first calculated by Laplace (1798) using Newton's laws of motion and of gravity. The variations were calculated in great detail, with suggestions for their climatic consequences, by the Yugoslav mathematician Milutin Milankovitch (1941). Fig 3.7 shows the three basic types of orbital variation that occur, discussed in detail by Berger (1984):-

(1) The eccentricity of the earth's orbit changes on timescales close to 10^5 years between values of about $e = 0$ and $e = 0.06$. The current value of e is 0.0167.

(2) The angle of tilt of the earth's spin axis ('the obliquity of the ecliptic') relative to the plane passing through all points on the earth's orbit (plane of the ecliptic) varies on a timescale close to 41×10^3 years. The angle is defined to be zero when the earth is imagined to be in an 'upright' position with its spin axis normal to the ecliptic. At present the angle, q , = 23.44° but fluctuates with variable amplitude between limits of about 22° and 24.5° and is at present decreasing on average by about $0.01^\circ/60$ years.

(3) The time of year when the earth is closest (perihelion) and furthest (aphelion) from the sun varies on timescales in the range $19-23 \times 10^3$ years. These changes are called the 'precession of the equinoxes' and are often measured by an angle, θ between the position of the earth in its orbit at the time of the N hemisphere autumn solstice and the position at perihelion. At present, the earth is at perihelion on approximately Jan 3rd so this angle is now 102° .

Fig 3.8 shows the computed changes in seasonal radiation at different latitudes for the last 10^6 years. Superimposed on these slow changes are much smaller, faster, changes in the geometry of the earth's orbit largely due to the orbit of Jupiter and variations in the moon's orbit which occur on timescales of decades to centuries (Fig 3.9) (Borisenkov et al (1983)).

Are these longer timescale (tens of thousands of years) radiation changes important? They are sufficient to alter the July radiation in the Northern Hemisphere through a range of at least 20% in most latitudes even though there is negligible change (0.2%) in the total

mean annual radiation. (Least average radiation is received when the orbit is circular). An increase of summer radiation would warm the summer climate, balanced of course by a decrease in winter radiation which should tend to cool the winter climate and so increase the seasonal contrast. Changes in atmospheric circulation should result: eg the monsoons might tend to be more vigorous if summer radiation is more intense in the Northern Hemisphere and the ITCZ might move further north. At present summer radiation is relatively weak, though not especially so. Although the earth is furthest from the sun in July, e is fairly low. Thus the earth does not get as far away from the sun in Northern Hemisphere summer at present as it did in some previous epochs. However if radiation decreases in summer and winters are still cold enough, some areas which lose their snow in summer when summer radiation is high may retain it when summer radiation is low. Albedo will increase and amplify any cooling effect. In this way snow fields and ice sheets might grow given other favourable circumstances.

A simple test calculation was carried out by Mason (1976) who showed that the deficiency of radiation in N Hemisphere summer between 83000 and 18000 BP may have been just enough to balance the latent heat of fusion produced between those dates, when the N Hemisphere ice sheets are thought to have expanded to their maximum size. He also calculated that the increase in summer radiation from 16000 BP to 6000 BP was just enough to provide the latent heat of fusion required to melt the amount of ice that is believed, from geological evidence, to have disappeared between these two dates (90% of the difference between the volume of ice-age ice and that which exists now). As Mason was at pains to point out, the calculation was over-simple and on their own the radiation deficiencies and excesses seemed insufficient to guarantee the waxing and waning of the ice sheets. On the other hand, the variations in summer radiation were of the correct order of magnitude to make a substantial contribution, given other favourable "positive feedback" processes. So it is very important to identify these other processes. On shorter timescales the 'Milankovitch' radiation changes are not entirely negligible; since the High Middle Ages (1200 AD) the flux of solar radiation incident on the atmosphere around the summer solstice at the North Pole has decreased by nearly 0.5%.

3.1.4 The equilibrium sensitivity of earth's climate to changes in S can be studied in an instructive if preliminary way using simple 'energy balance' models. Appendix I prepared by David Carson for the 1982 Advanced Lectures (attached to Lecture 9 of this series) discusses simple models and their approach to calculating the consequences of changes in S and in carbon dioxide. The results of many of these calculations are thought-provoking even if they turn out to be somewhat misleading. Figure 13 of Appendix I shows that a reduction of S by a few per cent might cause the earth to become completely glaciated; subsequent increase in S of at least 30% might be needed to melt the ice that has formed. These conclusions do indicate the potential sensitivity of climate to S in the presence of albedo feedback and the likely non-linearity of the response of the climate system.

In lecture 6 we shall discuss the effects of the Milankovitch radiation variations in more detail and the hypothesis that they are the pace-makers of the ice-age - interglacial fluctuations that have occurred quite regularly over the last 2-3 million years.

PART II - CARBON DIOXIDE AND THE GREENHOUSE EFFECT

3.2.1 Carbon dioxide is present in only small amounts in the atmosphere but is increasing by about 0.5% a year at present (current concentration is about 340 parts per million by volume (ppmv)). Carbon dioxide is important since it strongly absorbs long-wave radiation and re-emits it, so is radiatively very active in the climate system. The following discussion is only schematic and is oversimplified in many ways. It is adapted from Gill (1982) and applies to carbon dioxide, water vapour and other (lesser) 'greenhouse' gases.

Consider a greenhouse formed by placing a horizontal thin sheet of glass above the ground (Fig 3.10). Let this glass be nearly transparent to solar radiation (assume it absorbs a small fraction s), but much less transparent to terrestrial radiation. Suppose the glass and ground are initially cold. Let a downward flux, I , of solar radiation commence. Most of I will reach the ground; assuming the ground is a black body (ie has zero albedo), the ground will warm up to a temperature T_g and emit long-wave radiation with a flux U given by Stefan's law:-

$$U = \sigma T_g^4 \quad (1)$$

Now let a fraction e of U be absorbed by the glass. The glass will warm up and emit a flux of radiation B . Equilibrium is reached when on both sides of the glass the upward and downward fluxes of radiation are equal.

Thus

$$I = (1-e) U + B \quad \text{above the glass} \quad (2)$$

$$(1-s) I = U - B \quad \text{below the glass} \quad (3)$$

It is easy to show that

$$\sigma T_g^4 = I \left[\frac{1 - \frac{s}{2}}{1 - \frac{e}{2}} \right] \quad (4)$$

If s was zero and $e = 1$ then

$$\sigma T_g^4 = 2 I \quad \text{from (4)}$$

or $B = I$ so the flux received by the ground would be twice the solar flux.

T_g would increase by a factor $\Delta T_g = 2^{1/4} = 19\%$. Now s is about $1/5$ for present conditions and if this was true when $e = 1$ then $\Delta T_g = 16\%$. An increase in S of 19% would correspond to a surface temperature rise of about 50°C above the condition where $e=0$, if the albedo was zero; as the average amount of energy incident per unit area of the earth's surface is

about $I = 342 \text{ Wm}^{-2}$, and $\sigma = 5.7 \times 10^{-8} \text{ Wm}^{-2} \text{ K}^{-4}$, then $T_g = 278^\circ\text{K}$ and $\delta T_g = 53^\circ\text{C}$. In practice $T_g + \delta T_g$ would be considerably less than 331°K because $e < 1$ and importantly because of vertical atmospheric readjustments including the fact that some of I is converted to latent heat. (see Appendix I in Branch Memo. No. 173). This provides a 'radiative-convective' equilibrium ie the atmosphere above the ground takes up some of the extra heat initially absorbed at the surface.

Of course, the 'glass' is in reality distributed continuously in the vertical and water vapour is an important greenhouse gas which is very variable in concentration geographically (see Lecture 9). A point to note is that the addition of a greenhouse gas to the atmosphere does not necessarily leave the effective solar radiation received by the earth-atmosphere system unchanged eg if changes to the earth-atmosphere albedo also result. If we include the effect of the albedo A of the earth-atmosphere system and replace the net solar radiation received by the ground by $(1-s)(1-A)I$ (ignoring AS^2) and the net downward solar radiation above the glass by $I(1-A(1-s)^2)$ we obtain approximately:-

$$\sigma T_g^4 = \frac{I[1 - \frac{s+2A-3As}{2}]}{1 - e/2} \quad (5)$$

Here we arbitrarily attribute the albedo (due to ground and clouds) to the whole layer below the 'glass' so T_g is not really the ground temperature. If A decreases as e increases, σT_g^4 will increase at a faster rate. This could happen if snow and ice melted or low cloudiness decreased. Under present day conditions where nominally $T_g = 287^\circ\text{K}$, $s=0.2$ and $A = 0.3$, equation (5) gives approximately $e = 0.8$ for carbon dioxide, ozone, water vapour and other trace greenhouse gases together. Thus, schematically, at present $U = \sigma T_g^4 = 1.1I$ which implies that the long-wave radiation B incident on the ground from the atmosphere above is about $0.6I$. So $U-B = 0.5I$ at the surface. Figure 3.11 summarises the current radiation balance of the earth-atmosphere system. This shows that the direct net loss of long-wave radiation from the surface $U-B$ is $0.2I$, the remaining $0.3I$ being first converted to sensible and latent heat in the lower atmosphere and then lost as long-wave radiation (sensible heat) or once precipitation has occurred (latent heat).

Lecture 9 discusses the physical basis and evidence for the potential effects of carbon dioxide in the climate system in more detail and Lectures 6 and 7 indicate its possible role in past climatic changes.

PART III - Variations in volcanic dust in the stratosphere

3.3.1 From time to time huge volcanic eruptions of the explosive kind create world-wide veils of finely-divided dust causing optical effects such as a reddened sun or moon or halo effects around the sun like Bishop's rings. During an eruption, carbon dioxide and water vapour are ejected into the stratosphere with, very often, compounds of sulphur such as H₂S and SO₂ in gaseous form. The quantity of carbon dioxide ejected in a typical eruption is thought to be only about 0.01 ppmv, so the addition of carbon dioxide to the atmosphere is minute compared to the current rate of annual increase (1.5 ppmv). Likewise the heat output is, in relative terms, minute. It has long been considered that the dust vented from a huge volcanic eruption that reaches well into the stratosphere could affect climate. This was thought to be likely because:

(a) Estimates of surface temperature over widespread parts of the globe often showed a drop after (but also, disturbingly often, before) a huge volcanic eruption.

(b) The measured intensity of the direct solar beam was always reduced though the diffuse radiation usually increased to partially compensate.

The classic book on volcanic dust and climate is by Humphreys (1940), whose ideas are instructive and not wholly outdated. An extensive description of the development of observational studies of volcanic dust and climate effects is given by Lamb (1972). Fig 3.12, from Lamb (1972) shows examples of historical measurements of monthly average values of the strength of the direct solar beam, while Fig 3.13 shows a graph of historic worldwide average temperatures derived by Koppen (see p 410 of Lamb (1972)). The timing of the largest volcanic eruptions is shown on the diagrams. Lamb has devised a "dust veil" index to measure the climatologically most important eruptions. The index is partly based on observations of the optical effects of the dust but also on the worldwide fall in surface temperature (as far as it can be judged) following a given eruption (Lamb (1970)). This subjective index suggests that the eruptions of Tambora (1815) (Indonesia), Coseguina (1835) (Nicaragua), Krakatau (Indonesia) (1883) and Agung (Indonesia) (1963) (Fig 3.14) were among those most likely to have affected surface temperatures since the beginning of the nineteenth century, prior, that is, to the recent eruption of El Chichon (see later). On a millennial time scale, Fig 3.15, from Lamb (1972), shows an apparent association between the reconstructed extent of sea-ice near Iceland and volcanic eruptions in Iceland.

3.3.2 Controversy concerning volcanic dust and climate

The problem of whether the apparent associations between volcanic activity and climate exist continues to be controversial. The main reasons for controversy are:-

(a) There is sufficient uncertainty about the physics of the interaction between volcanic dust and solar and terrestrial long wave radiation that the sign of the effect of stratospheric volcanic dust on surface temperature is uncertain and may vary from eruption to eruption.

(b) The net effects depend crucially on the size distribution and chemical constitution of the dust, which may vary between eruptions.

(c) It has not yet proved possible to use an AGCM with a realistic stratosphere and using what would now be regarded as the essential physics of the radiative interactions, to attempt to simulate the climatic effects of volcanic dust. In any case, the simulated response of the oceans could be crucial as volcanic 'dust' may stay in the stratosphere for several years.

It is now thought that the reason why past ground measurements have indicated long-residence times for stratospheric dust, despite the appreciable scavenging that must exist due to dynamical interactions between troposphere and stratosphere, concerns the fact that some of the "dust" is formed after the eruption. Sulphur gases (H_2S , SO_2 etc) formed during the eruption may slowly combine with stratospheric water vapour to produce reflective, aqueous droplets of a typical diameter $1 \mu m$ or less whose terminal velocities are very low. So the quantity of sulphur gas and possibly sulphur particles ejected in an eruption is now thought to be very important. Lamb (1972) shows terminal velocities for spherical particles of several radii (Table 3.3.1).

Table 3.3.1 (from Lamb (1972))

Stratospheric residence times for volcanic dust
(Total times taken to fall through still air to tropopause at (a) 17 km,
(b) 12 km)

Particle Diameter	Initial height (km)	Residence time	
		(a)	(b)
2 μm	40	25 weeks	41 weeks
	30	21 weeks	37 weeks
	25	16 weeks	31 weeks
	20	7 weeks	23 weeks
1 μm	40	1.9 years	3.1 years
	30	1.6 years	2.8 years
	25	1.3 years	2.4 years
	20	0.6 years	1.7 years
0.5 μm	40	7.8 years	12.5 years
	30	6.5 years	11.3 years
	25	5.0 years	9.7 years
	20	2.2 years	6.9 years

3.3.3 El Chichon

In April 1982 a very violent, explosive eruption occurred in S Mexico from the volcano El Chichon (the "lump on the head") situated at 17°N 93°W. Fig 3.16 from Robock and Matson (1983) shows how the dust from that explosion circled the globe in about 1 month in a narrow band between 15°-25°N. Winds were easterly, and accelerating, at the 25-30 km level where much of the dust initially resided because the summer stratospheric circulation was just getting underway. At Hawaii (Central Pacific 19°N) directly under the dust cloud, direct solar radiation was reduced by up to 30% in the months following the eruption, a reduction offset, but not completely, by an increase in diffuse solar radiation. (Coulson et al (1982)). The measurements indicated that in the visible spectrum at a wavelength of 0.55 μm the dust produced a mean optical depth T of 0.25. Optical depth is defined as

$$F = F_0 e^{-T}$$

F_0 is the incident flux and F is that part of the flux that emerges below the dust layer without absorption or being scattered ie F only measures the reduction of direct radiation. Balloon and other measurements suggested that a few months after the eruption much of the cloud was composed of droplets containing 75% sulphuric acid and 25% water with a mode radius of about 0.3 μm (MacCracken and Luther (1984) give details). By July the dust cloud, now at a height of between 20-25 km, reached Italy and became visible to the naked eye on a few evenings in August 1982 around Bracknell, with some unusual sunsets. Referring back to Table 3.3.1, droplets near a radius of 0.3 μm have such very low terminal velocities so that dynamical and other processes are likely to be important for their removal from the stratosphere. It has yet to be shown that El Chichon has affected global surface temperatures (which in fact rose soon after the eruption, because of El Nino (see lecture 5)).

3.3.4 Heating of stratospheric dust layer

It is not completely obvious that a stratospheric volcanic dust cloud should get hotter than its environment. The particles may be so small that solar heating is negligible and their radiative properties could be such that infra-red radiation from below also has little effect. Newell (1981) claimed to have detected a heating of the dust cloud produced by Agung (1963) by several degrees centigrade. Theoretical work has recently suggested that a heating of several degrees is possible for the likely sizes and chemical constituents of volcanic dust, mainly due to the absorption of infra-red radiation from below. Parker and Brownscombe (1983) cautiously concluded that the El Chichon dust cloud was heated near the equator between 30-50 mb by several degrees centigrade. Fig 3.17A (from Parker and Brownscombe (1983)) shows stratospheric temperatures at several levels in 1980-82 derived from the NOAA 6 Stratospheric Sounding Unit and Microwave Sounding Unit. Of the levels sampled, that at 50 mbar shows the largest temperature increase from 1981-82. Fig 3.17B, (again from Parker and Brownscombe) shows the 30 mb temperature anomalies in August 1982 from radiosonde data. A complicating factor in this and the Agung studies is that anomalous warming was expected in both 1963 and 1982 within 15°N or S of the equator below the descending, westerly, phase of the stratospheric "quasi-biennial oscillation" (QBO) (see Lecture 5). An

analysis by Labitzke et al (1983) of the 50 and 30 mbar temperatures between 1964 and 1982 strongly suggests that the QBO contributed only a part of the 1982 warming. Nevertheless the observed temperature anomaly maximum near the equator in Fig 3.17B, rather than at the latitude of the main dust cloud (20°N), is probably a result of the additional influence of the QBO.

3.3.5 A schematic, simplified, model of effects of volcanoes on surface temperature

Although literature on the modelling of the physical effects of volcanic dust on the surface temperature is in some disagreement, there is an emerging picture of the important physical processes. However the sign of the effect of volcanic dust in the surface energy balance is difficult to determine because there are two important competing physical effects and a host of smaller ones. The most important opposing effects are:-

- (a) The dust layer reflects solar radiation, tending to cool the surface of the earth.
- (b) The dust layer absorbs terrestrial radiation, tending to warm the surface of the earth.

Absorption of solar radiation can be significant but is now thought to be fairly small, at least in some volcanic eruptions.

Fig 3.18 shows a simple schematic model (which cannot be used to make predictions). Because we shall estimate the perturbation of the surface energy balance due to stratospheric dust, we will not explicitly include the effects of carbon dioxide and other greenhouse gases which are assumed to be fixed. Imagine solar radiation I passing down through the dust layer; a fraction rI is reflected to space and lost while the remaining fraction $tI = (1-r)I$ is transmitted to ground either as direct or diffuse radiation. Here we have assumed no absorption of solar radiation by the dust layer itself, which is not quite correct. The transmitted radiation, I_t , reaches the "ground" and a fraction $A I_t$, is reflected upward (in principle A is not quite the same as for the "non dust" case as more of the solar radiation is diffuse and less is direct). On reaching the dust layer again, an amount of reflected radiation $t(A I_t)$ is lost and an amount $r(A I_t)$ is reflected down. So the initially reflected solar radiation is multiply-reflected between dust layer and ground with rapidly decreasing intensity. The initial loss of solar radiation to the system, rI , is to some extent "made up" by the multiple reflections as the expected radiation loss from the ground in the absence of dust (for a finite non-zero value of A) is clearly reduced. However the total radiation absorbed by the ground cannot quite reach the initial amount transmitted (I_t) for a finite value of A .

Now also assume that a fraction b of the long-wave radiation U lost from the surface (partly indirectly from the troposphere itself - see section 2) is absorbed by the dust layer without further reflection.

Then we find that the solar radiation absorbed by the ground I_G is:-

$$I_G = (1-A)tI (1+rA+r^2A^2+\dots)$$

or
$$I_G = \frac{(1-A)tI}{1-rA}$$
 after summation

Similarly the solar radiation lost through the dust layer to space after multiple reflection is:-

$$I' = rI + t^2AI [1+rA+\dots]$$

or
$$I' = rI \left[\frac{1+t^2AI}{1-rA} \right]$$

We can now calculate the value of I_G . The radiation balance at the ground is:-

$$-B+U = I_G \quad (1)$$

The radiation balance above the dust layer is

$$B+(1-b)U = I-I' \quad (2)$$

Adding (1) and (2) and substituting for I_G and I' we find

$$U = \left[\frac{2}{2-b} \right] I \left[\frac{1-r-A+Ar}{1-rA} \right] \quad (3)$$

Now if $t = 1$ and $r = 0$, ie no dust layer exists, we found in section 3.1.1 that $U = (1-A)I$. So the net change ΔU in the long-wave radiation lost (eventually) by the ground when a dust layer is interposed is:-

$$\Delta U = I(1-A) \left\{ \left[\frac{1+\frac{b}{2}}{1-rA} \right] (1-r) - 1 \right\} \quad (4)$$

Now $U = \sigma T_g^4$ (approximately) as in section 3.2.1, so $\Delta U = 4\sigma T_g^3 \Delta t_g$. Table 3.3.2 shows calculations of equilibrium values of Δt_g , assuming $t_g = 287^\circ\text{C}$, for reasonable values of t and b (where of course the effects of additional surface evaporation etc are neglected). MacCracken and Luther (1984), Pollack et al (1976) and Chou et al (1984) give a discussion of the detailed physics and its uncertainties and suggestions for values of t , (dust layer transmission coefficient), and b (dust layer absorption coefficient) and their effects on surface temperature.

TABLE 3.3.2 EQUILIBRIUM TEMPERATURE CHANGES AT THE SURFACE FROM THE SCHEMATIC MODEL, °C

1.	b = 0			
		t = 0.99	t = 0.97	t = 0.95
	A			
	0	-0.6	-1.9	-3.1
	0.3	-0.3	-0.9	-1.6
	0.6	-0.1	-0.3	-0.5
	0.8	0.0	-0.1	-0.1
2.	b = 0.02			
	A	t=0.99	t=0.97	t=0.95
	0	0.0	-1.3	-2.6
	0.3	0.1	-0.5	-1.1
	0.6	0.2	-0.3	-0.3
	0.8	0.1	+0.1	0.0

Even if the magnitudes are incorrect, it is seen that the sign of the change in surface temperature is very sensitive to t and to b and also to A . These results qualitatively agree with existing ideas, despite the crudeness of the model. So a cooling due to volcanic dust is less likely where A is high but small changes in b , the coefficient that measures the absorption by the dust of long-wave radiation, can easily change the sign of a surface temperature response. Chou et al (1984) agree that eruptions are likely to produce varying surface temperature responses due to differences in particle size or chemical composition even if their dust clouds are similar in extent and optical depth. Also, the temperature changes in Table 3.3.2 would also usually be much reduced near the surface due to the thermal inertia of the oceans; so bigger temperature changes are more likely higher in the atmosphere. Fig 3.19 from Chou et al (1984) is a simple (but very uncertain) calculation allowing for these effects. In Lecture 8 we briefly consider whether it is likely that volcanic dust has really affected surface and tropospheric temperature since about 1850.

LECTURE 3 - REFERENCES

- BERGER, A (1984) Accuracy and frequency stability of the Earth's orbital elements during the Quaternary. *Milankovitch and Climate, Pt. I*: Ed. A Berger et al, NATO ASI 126, (D. Reidel Pub. Co.), pp 3-39.
- BERGER, A and PESTIAUX, P (1984) Accuracy and stability of the Quaternary terrestrial insolation. *Milankovitch and Climate Pt 1*. Ed: A Berger et al, NATO ASI, 126, (D. Reidel Pub. Co.), pp 83-111.
- BORISENKOV, YE. P, TSVETKOV, A V and AGAPONOV, S V (1983) On some characteristics of insolation changes in the past and the future. *Climatic Change*, 5, pp 237-244.
- CALDER, N (1974) *The Weather Machine*. BBC, London.
- CHOU, M-D, PENG, L, and ARKING, A (1984) Climate Studies with a multilayer energy balance Model, Pt III: Climatic impact of stratospheric volcanic aerosols. *J. Atm. Sci.*, 41, pp 759-767.

COULSON, K L, DEFOOR, T E and DELUISI, J (1982) Lidar and Optical Polarization Measurements of Stratospheric Cloud in Hawaii. Presented at the Fall AGU Meeting, San Francisco, Dec 7-15 1982, Eos, 63, p 897.

EDDY, J A (1983) A Historical review of solar variability weather and climate. In 'Weather and Climate Responses to solar variations'. Ed: B.M. McCormac, Colorado Ass. Univ. Press., pp 1-15.

GILL, A E (1982) Atmosphere-ocean dynamics. Academic Press.

GILLILAND, R L (1983) Climate change as a test of the influence of external perturbations. In 'Weather and Climate responses to solar variations'. Ed: B M McCormac, Colorado Ass. Univ. Press, pp 273-281.

HUDSON, H S (1983) Variations of the Solar Radiation Input. In 'Weather and Climate responses to solar variations'. Ed: B M McCormac, Colorado Ass. Univ. Press. pp 31-41.

HUMPHREYS, W J (1940) Physics of the air. 3rd Edition. Reprinted by Dover (1964).

KOPPEN, W (1873) Ueber Mehrjahrigere Perioden der Witterung, insbesondere uber die 11-jahrigere Periode der Temperatur. Z. Met., Vienna, 8, pp 241-248, 257-267.

KOPPEN, W (1914) Lufttemperaturen, Sonnenflecke und vulkanausbruche. Met., Z. Braunschweig, 31, pp 305-328.

LABITZKE, K, NAUJOKAT, B, and McCORMICK, M P (1983) Temperature effects on the stratosphere of the April 4, 1982, eruption of El Chichon, Mexico. Geophys. Res. Letters, 10, pp 24-26.

LAMB, H H (1970) Volcanic dust in the atmosphere. Phil Trans, Roy Soc, A, 266 (No 1178) pp 426-533.

LAMB, H H (1972) Climate, Present, Past and Future. Vol 1, Methuen.

MacCRACKEN, M C and LUTHER, F M (1984) Radiative and climate effects of the El Chichon eruption. Proc of Fifth Amer. Met. Soc. Conf. Radiation, 31 October-4 November 1983, Baltimore MD.

MASON, B J (1976) Toward the understanding and prediction of climatic variations. Q.J. Roy. Met. Soc., 102, pp473-498.

MILANKOVITCH, M (1941) Canon of insolation and the ice age problem - Spec. Pub. 132, Trans. No. 1793, 1969 - Israel Program for Scientific Translations.

NATIONAL RESEARCH COUNCIL (1982) Solar Variability, Weather and Climate. Ed: J Eddy. Studies in Geophysics Ser., Geophys. Res. Board. National Academy Press.

NEWELL, R E (1981) Further studies of the atmospheric temperature change produced by the Mt Agung volcanic eruption in 1963. J. Volcanology and Geoth. Res., 11, pp 61-66.

PARKER, D E and BROWNSCOMBE, J L (1983) Stratospheric warming following the El Chichon volcanic eruption. *Nature*, 301, pp 406-408.

POLLACK, J B, TOON, O B, SAGAN, C, SUMMERS, A, BALDWIN, B, and VAN CAMP, W (1976) Volcanic Explosions and Climatic Change: A theoretical assessment. *J. Geophys. Res.*, 81, pp 1071-1083.

RAMPINO, M R and SELF, S (1982) Historic eruptions of Tambora (1815), Krakatau (1883), and Agung (1963), their stratospheric aerosols, and climatic impact. *Quart. Res.*, 18, pp 127-143.

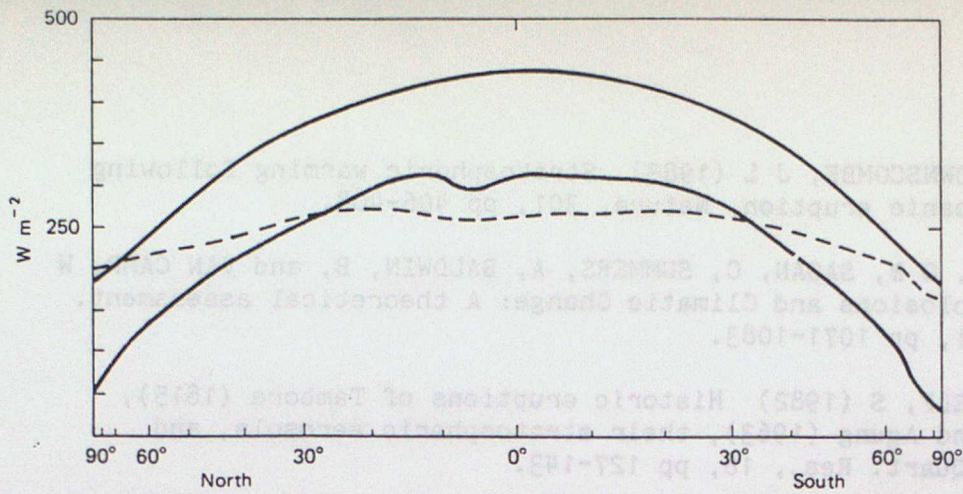
RASCHKE, E, VONDER HAAR, T H, BANDEEN, W R and PASTERNAK, M (1973) The annual radiation balance of the earth-atmosphere system during 1969-70 from Nimbus 3 measurements. *J. Atm. Sci.*, 30, pp 341-364.

ROBOCK, A and MATSON, M (1983) Circumglobal Transport of the El Chichon volcanic dust cloud. *Science*, 221, pp 195-197.

STEPHENS, G L, CAMPBELL, G G and VONDER HAAR, T H (1981) Earth radiation budgets. *J. Geophys. Res.*, 86, C10, pp 9739-9760.

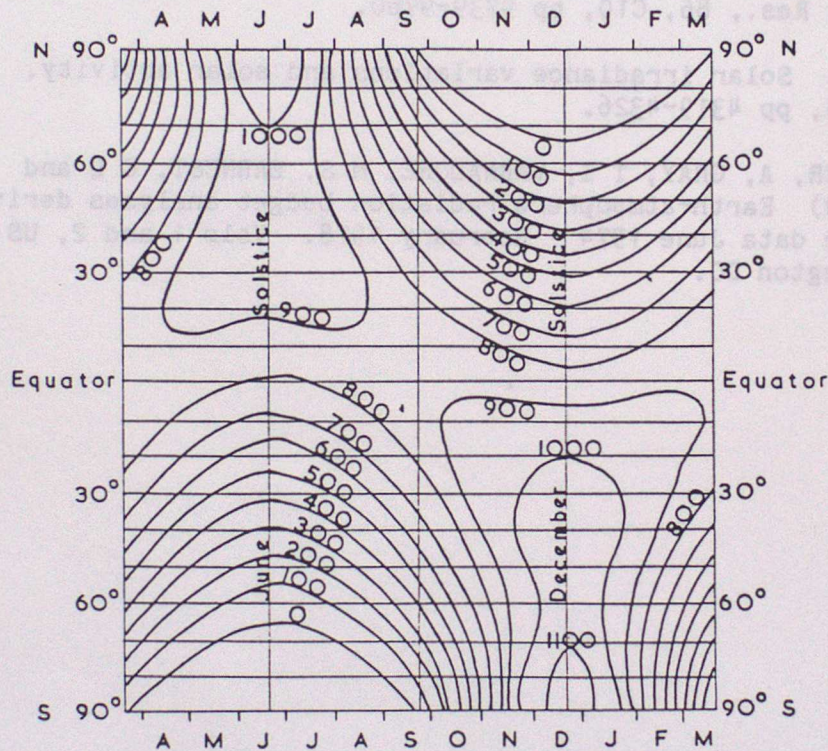
WILLSON, R C (1982) Solar irradiance variations and solar activity. *J. Geophys. Res.*, 87, A6, pp 4319-4326.

WINSTON, J S, GRUBER, A, GRAY, T I, VARNADORE, M S, EARNEST, C L and MANNELLO, L P (1979) Earth-atmosphere radiation budget analyses derived from NOAA satellite data June 1974 - February 1978. Vols 1 and 2, US Dept of Commerce, Washington DC.



The radiation balance of the earth. The upper solid curve shows the average flux of solar energy reaching the outer atmosphere. The lower solid curve shows the average amount of solar energy absorbed; the dashed line shows the average amount of outgoing radiation. The lower curves are average values from satellite measurements between June 1974 and February 1978, and are taken from Volume 2 of Winston *et al.* (1979). Values are in watts per square meter. The horizontal scale is such that the spacing between latitudes is proportional to the area of the earth's surface between them, i.e., is linear in the sine of the latitude.

Figure 3.1A From Gill (1982)



Daily totals of solar radiation available in different latitudes of the Earth in the absence of the atmosphere, in g cal/cm^2 , around the year, at the present epoch.

Figure 3.1B From Lamb (1972)

ANNUAL ALBEDO

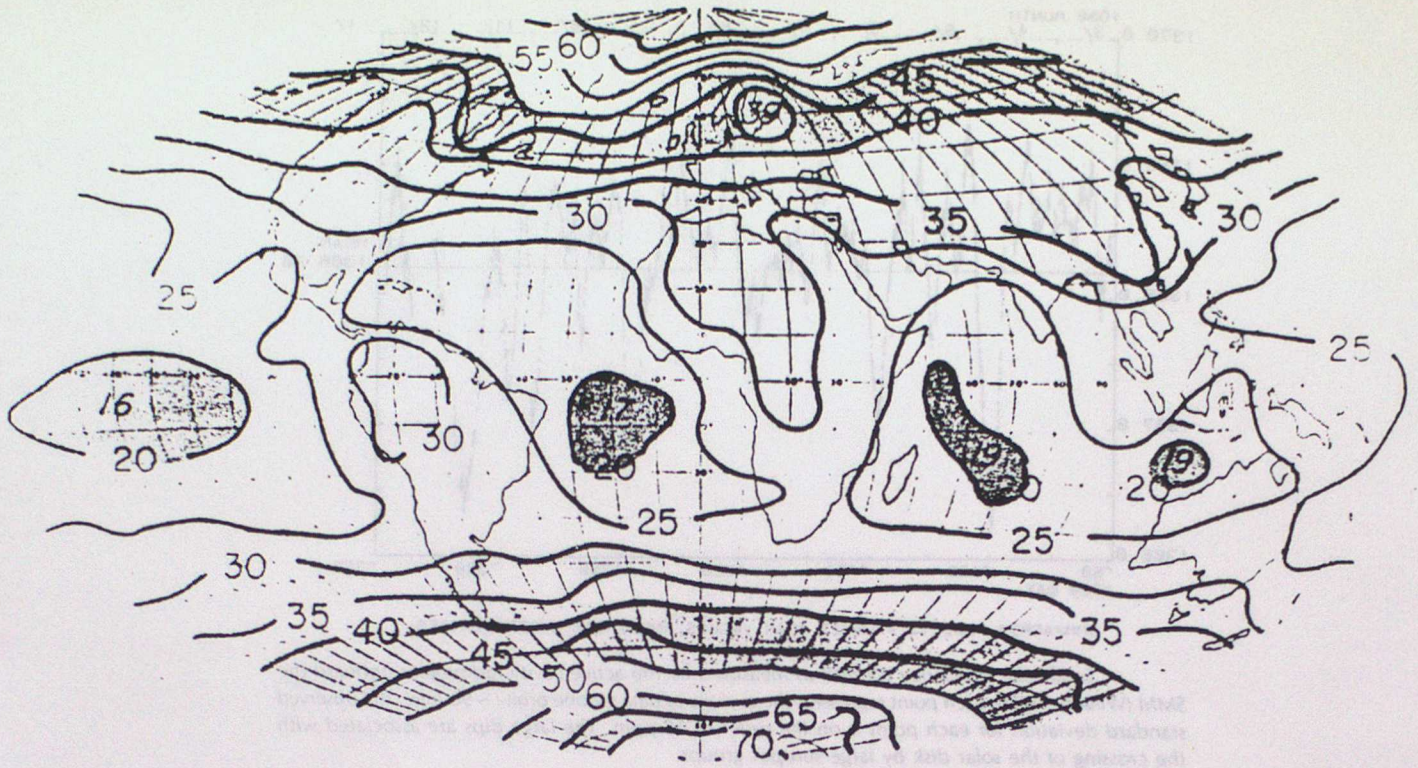


Figure 3.2 The average albedo obtained from a composite of 48 months of satellite data obtained between 1964 and 1977. From Stephens et al (1981)

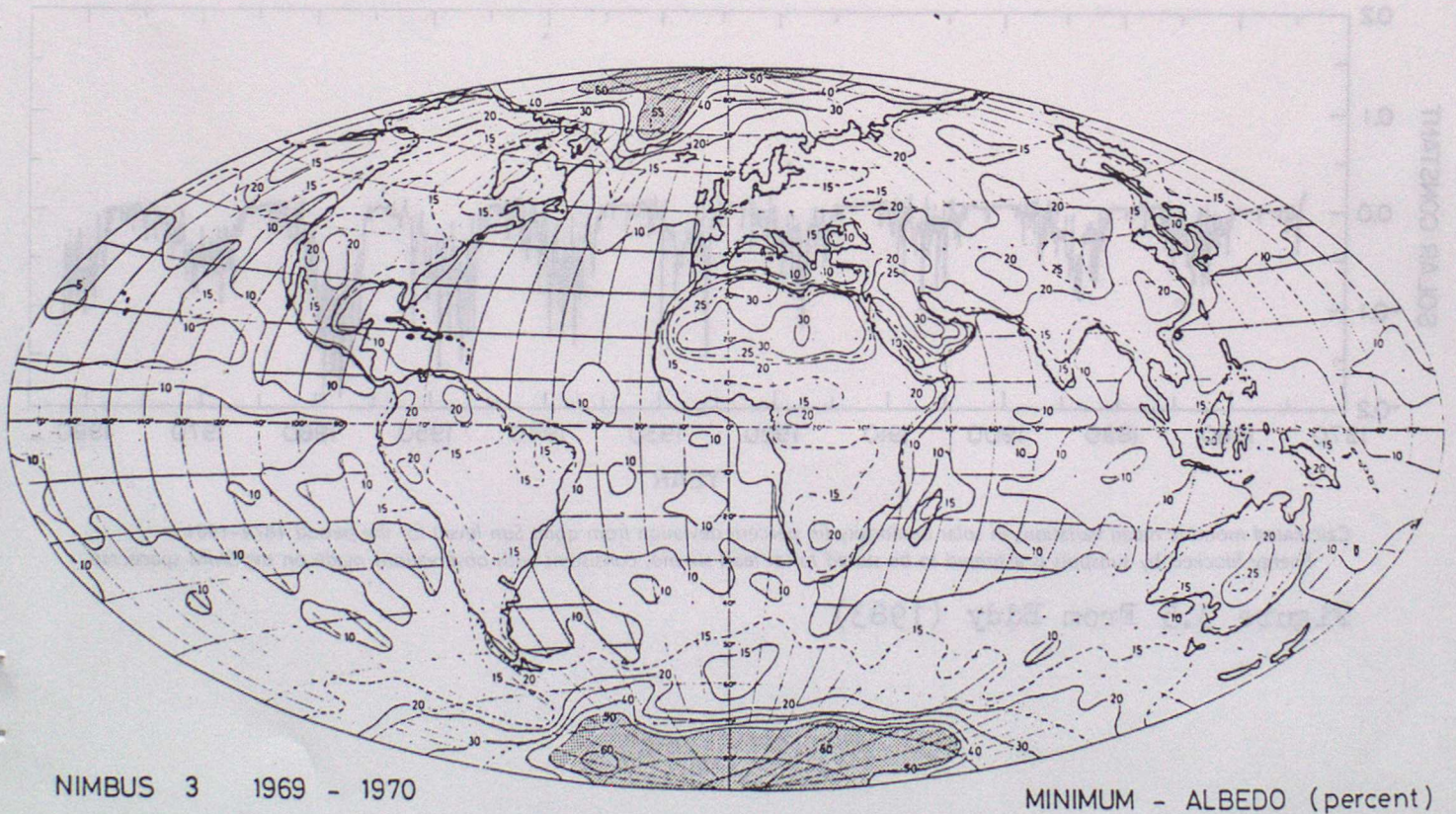
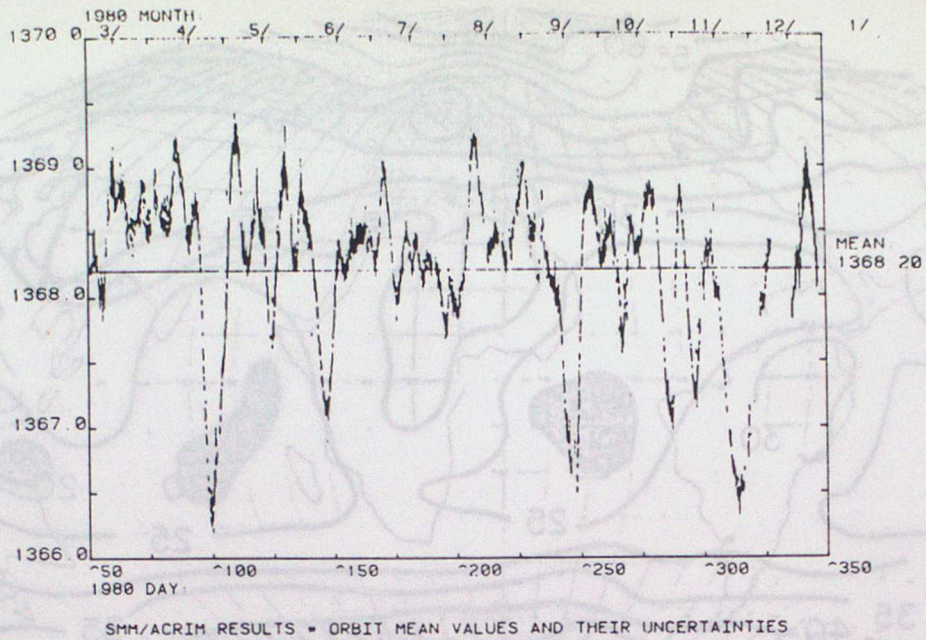
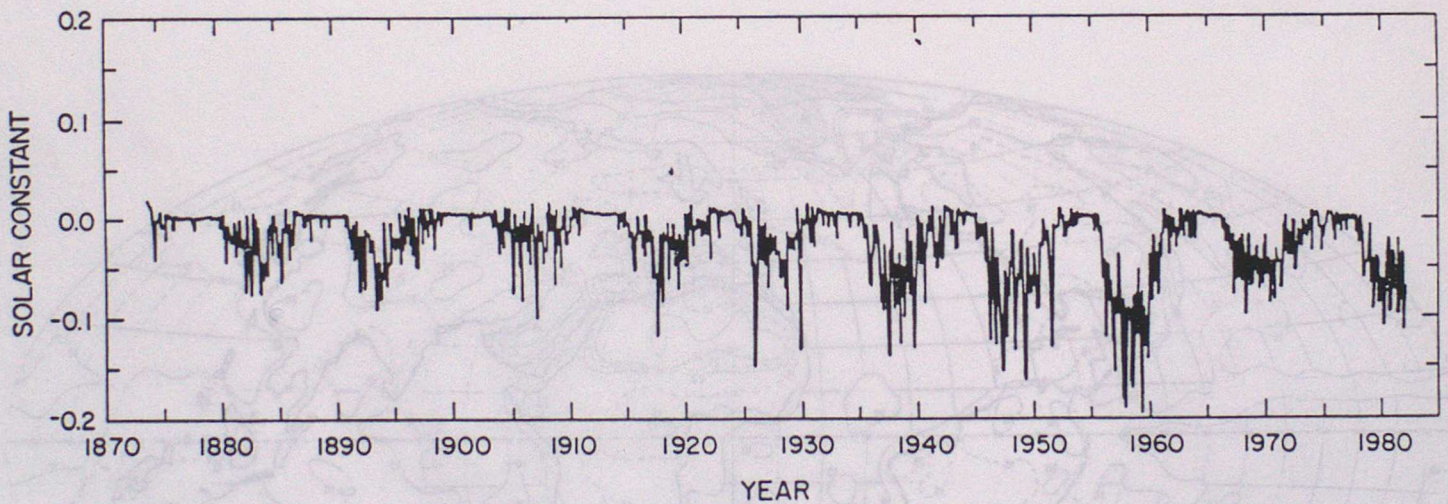


Figure 3.3 The minimum albedo of the Earth from Nimbus3 satellite measurements in 1969 to 1970. From Raschke et al (1973)



Total solar irradiance ($W m^{-2}$) as measured by the active cavity radiometer onboard the SMM (Willson, 1982). Each point represents the average of data for one orbit (~96 min); the observed standard deviation for each point is on the order of 15 ppm. The large dips are associated with the crossing of the solar disk by large sunspot groups.

Figure 3.4 From Hudson (1983)

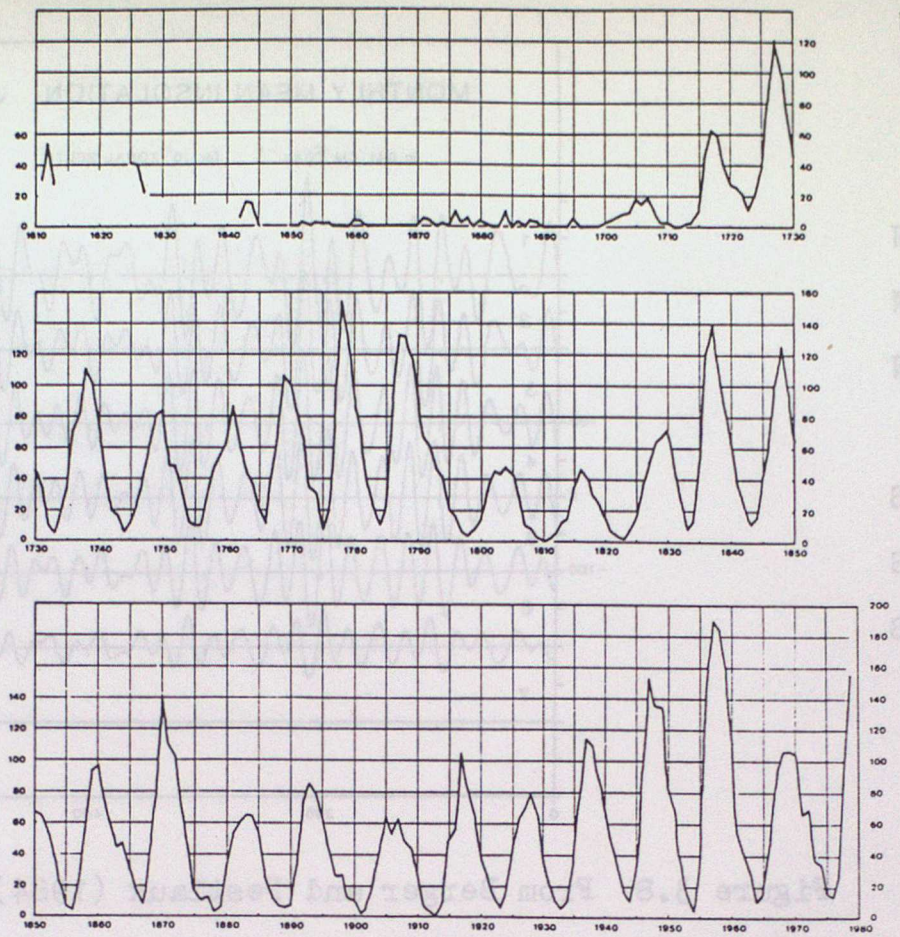


Calculated monthly mean variations in solar luminosity (in percent deviation from quiet Sun level) for the period 1874-1981. Energy blocked by sunspots is assumed to be stored for at least six mo, consistent with observations made on the SMM spacecraft.

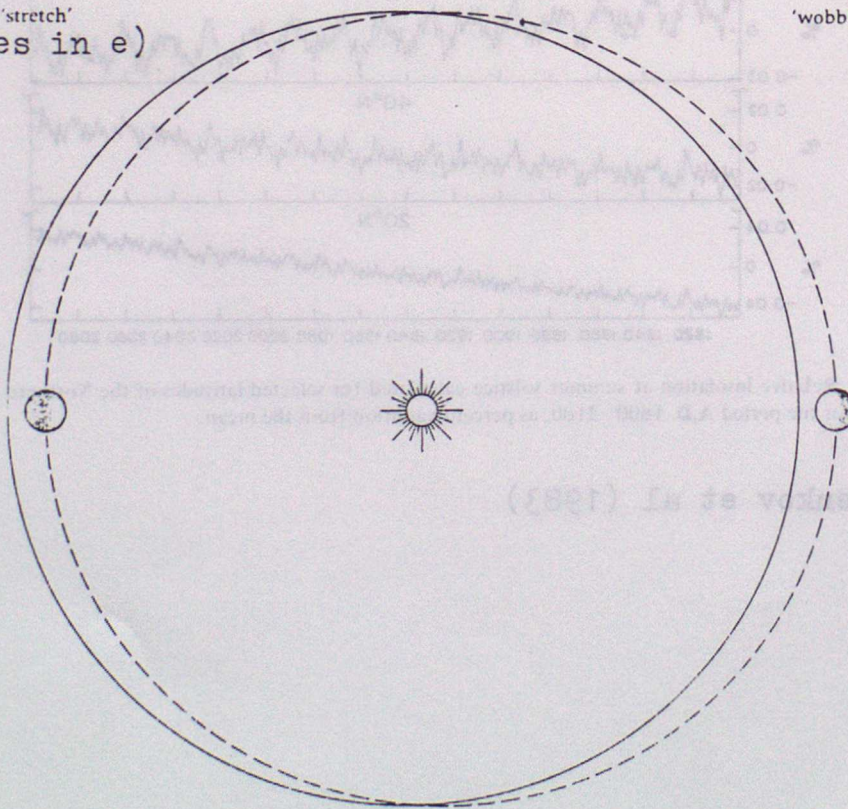
Figure 3.5 From Eddy (1983)

Annual mean sunspot numbers, 1610-1979. During the Maunder Minimum, solar activity (as measured by sunspot number) fell to an unprecedented low level for approximately 70 years centered about 1670

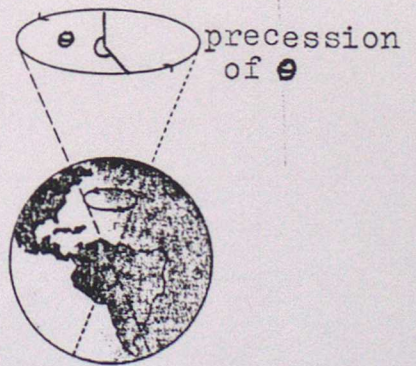
Figure 3.6
From National Research
Council (1982)



'stretch'
(changes in e)



'wobble'



'roll' - changes in q

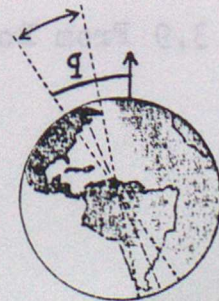


Figure 3.7 From Calder (1974)

- 1=85°N
- 2=55°N
- 3=25°N
- 4=5°N
- 5=25°S
- 6=55°S
- 7=85°S

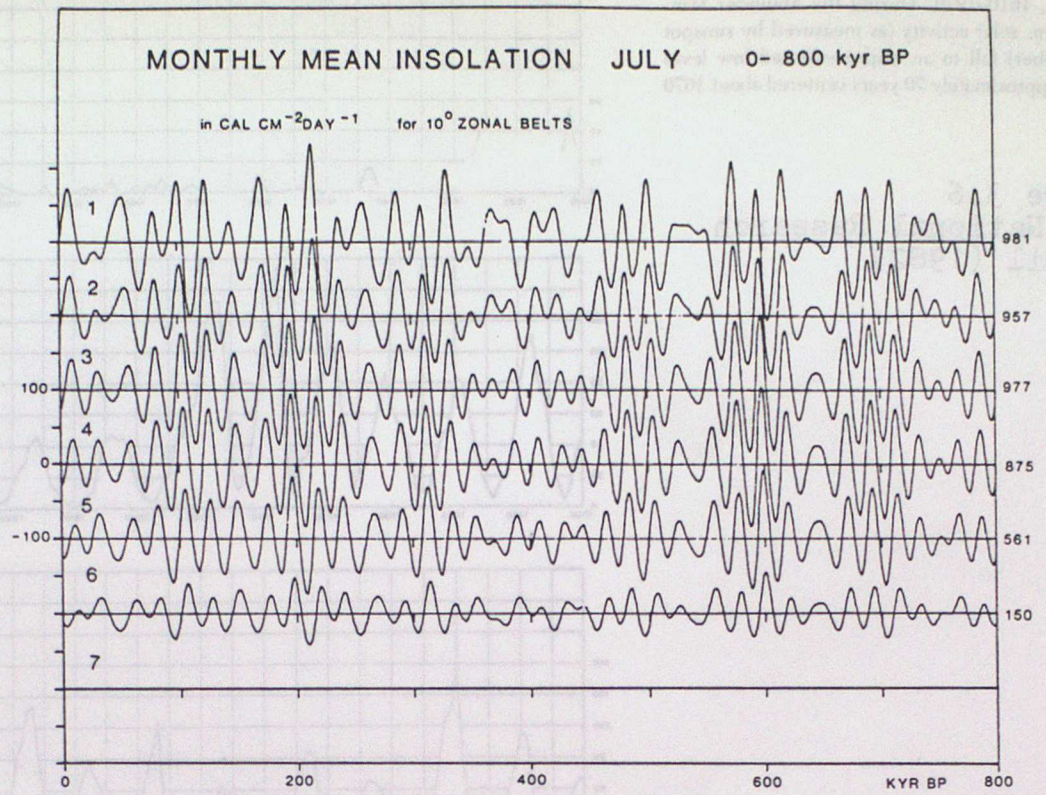
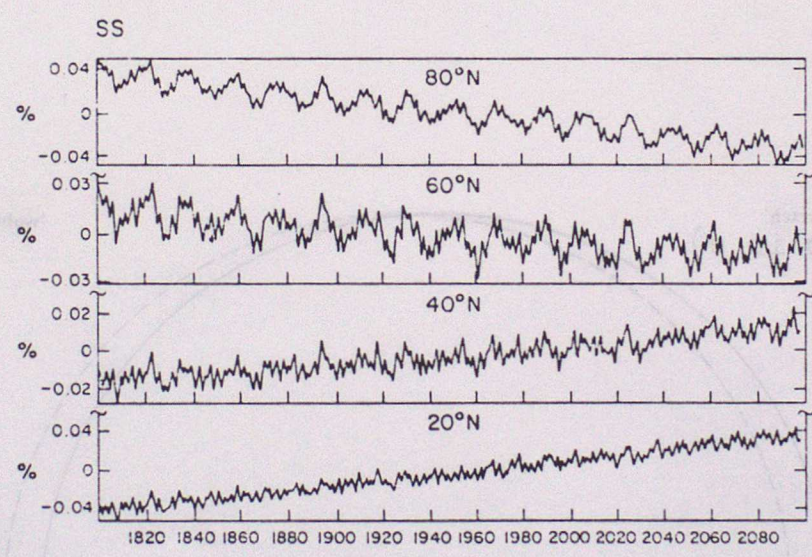


Figure 3.8 From Berger and Pestiaux (1984)



Relative insolation at summer solstice calculated for selected latitudes of the Northern Hemisphere for the period A.D. 1800-2100, as percent variation from the mean.

Figure 3.9 From Borisenkov et al (1983)

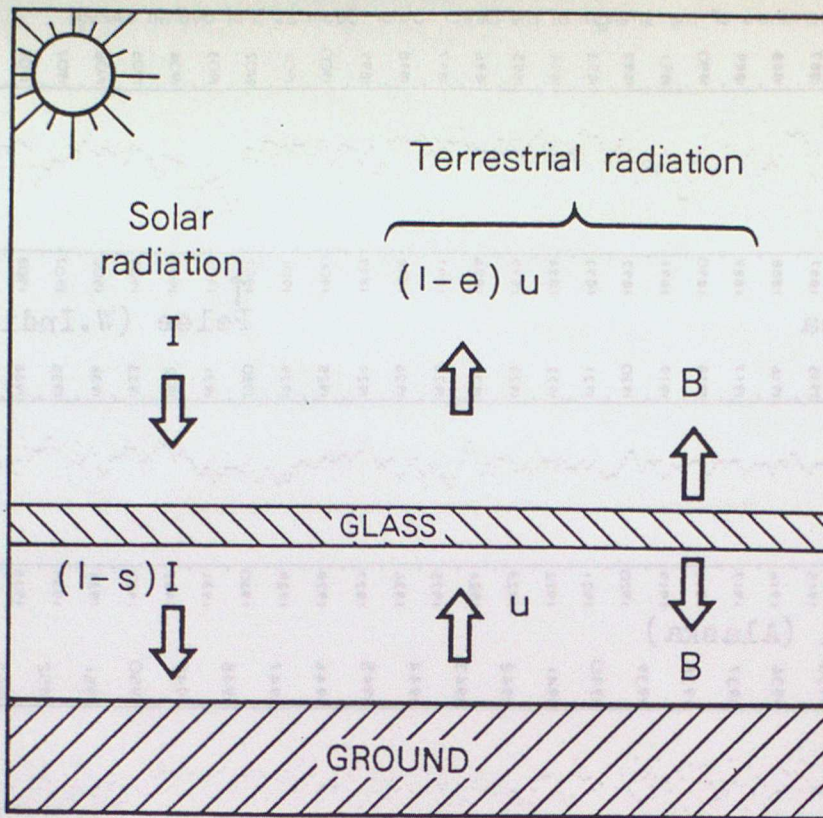
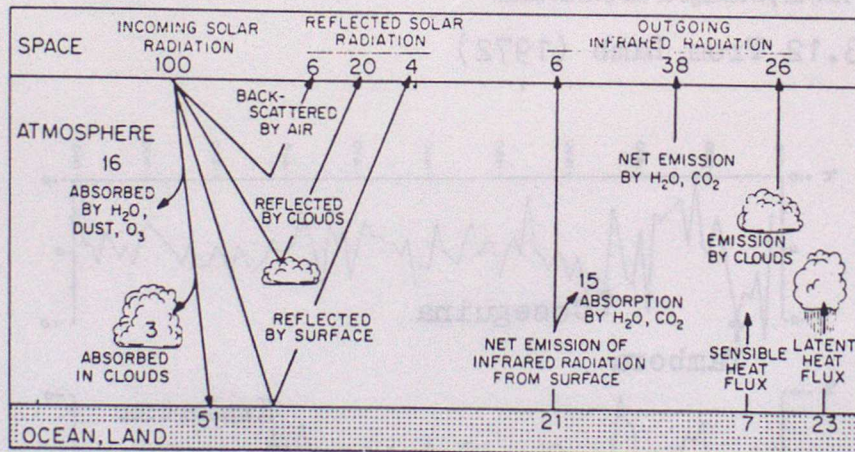


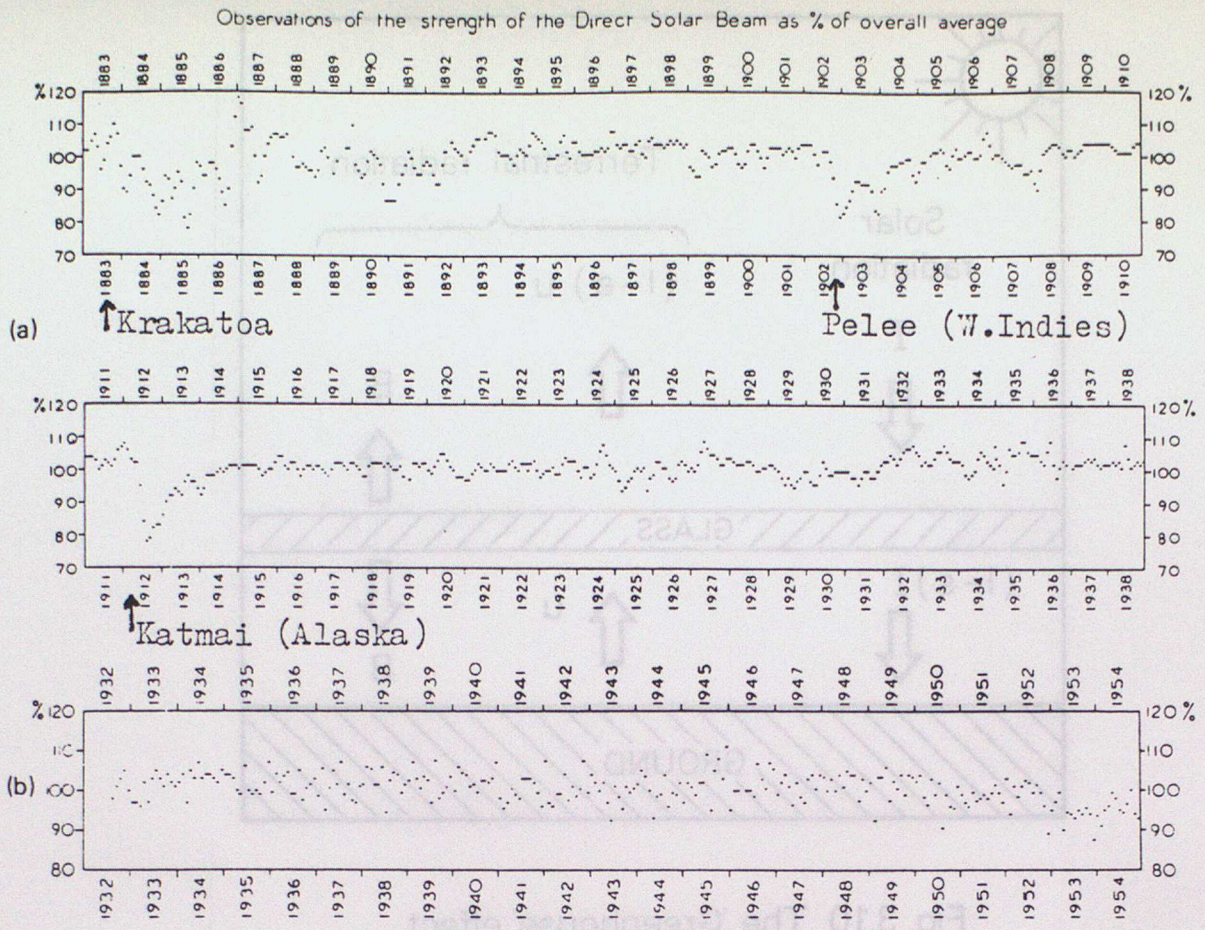
Fig. 3.10 The 'Greenhouse' effect

Adapted from Gill (1982)



Radiation balance for the atmosphere. [Adapted from "Understanding Climatic Change," U.S. National Academy of Sciences, Washington, D.C., 1975, p. 14, and used with permission.]

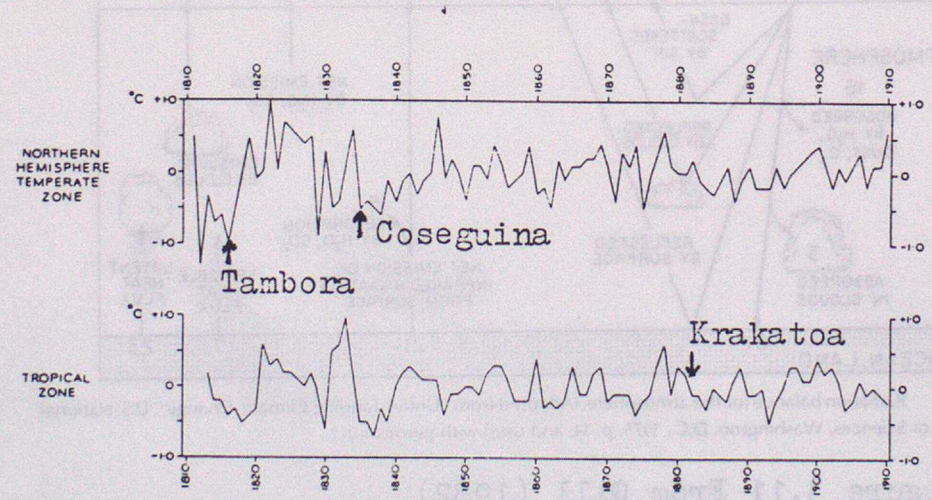
Figure 3.11 From Gill (1982)



(a) Average monthly values of the strength of the direct solar radiation derived from observations at mountain observatories between 30° and 60°N in America, Europe, Africa and India from 1883 to 1938, as percentage of the overall mean.

(b) Average monthly values of the strength of the direct solar radiation derived from observations at Matsumoto (36°15'N, 137°58'E) and Shimizu (32°47'N, 132°58'E) in southern Japan from 1932 to 1954, as percentage of the overall mean.

Figure 3.12 From Lamb (1972)



Anomalies of yearly mean surface temperature averaged for certain areas, from 1815 to 1910:

(a) Northern hemisphere temperate zone

(b) Tropical zone

Unsmoothed yearly values.

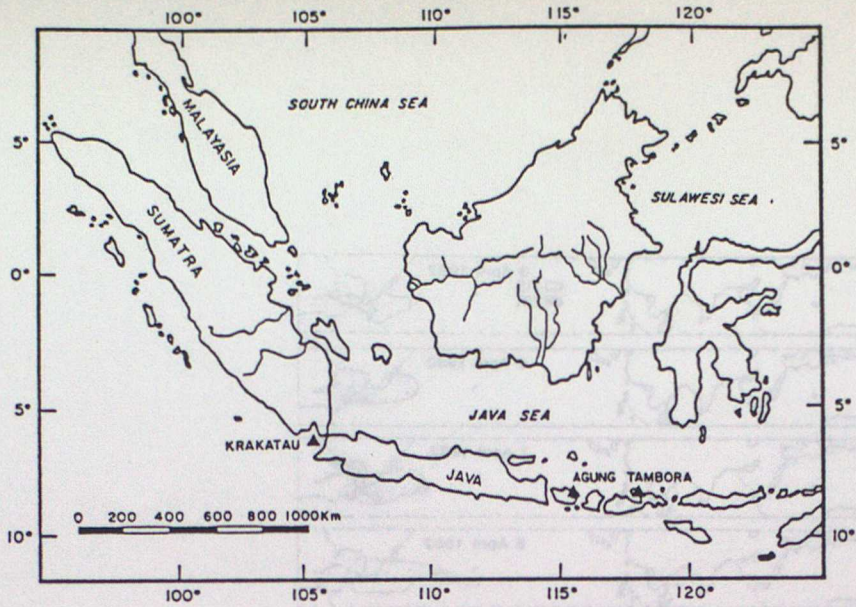
Standard deviations of the yearly values here plotted:

Northern temperate zone (land stations) 0.38°C.

Tropical zone (land stations) 0.29°C.

(After KÖPPEN 1873, 1914.)

Figure 3.13 From Lamb (1972)



Map showing location of the three Indonesian eruptions discussed here: Tambora (1815), Krakatau (1883), and Agung (1963). (triangles).

Figure 3.14 From Rampino and Self (1982)

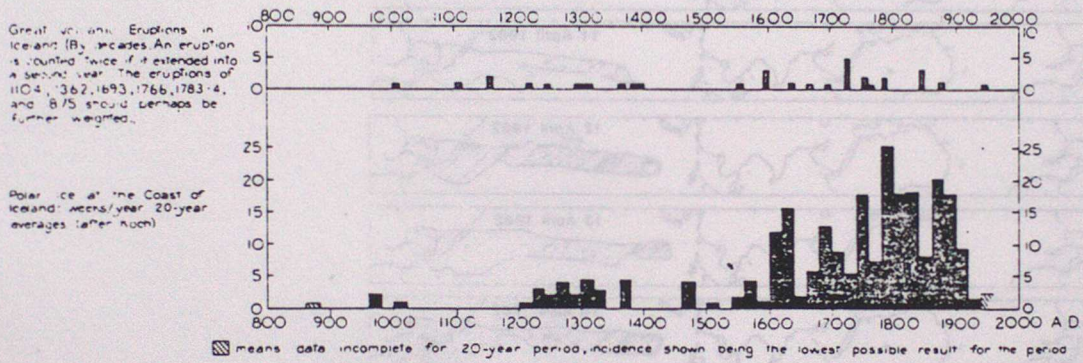


Figure 3.15 From Lamb (1972)

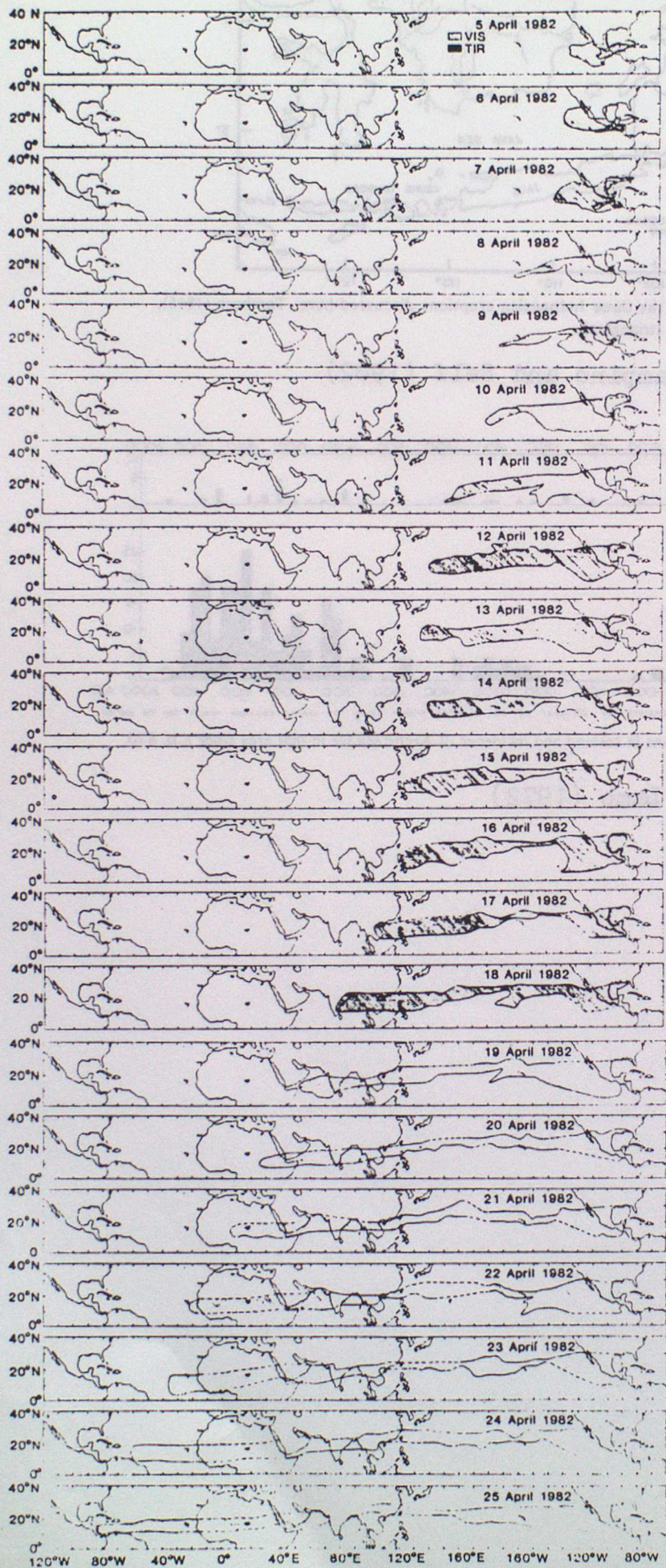
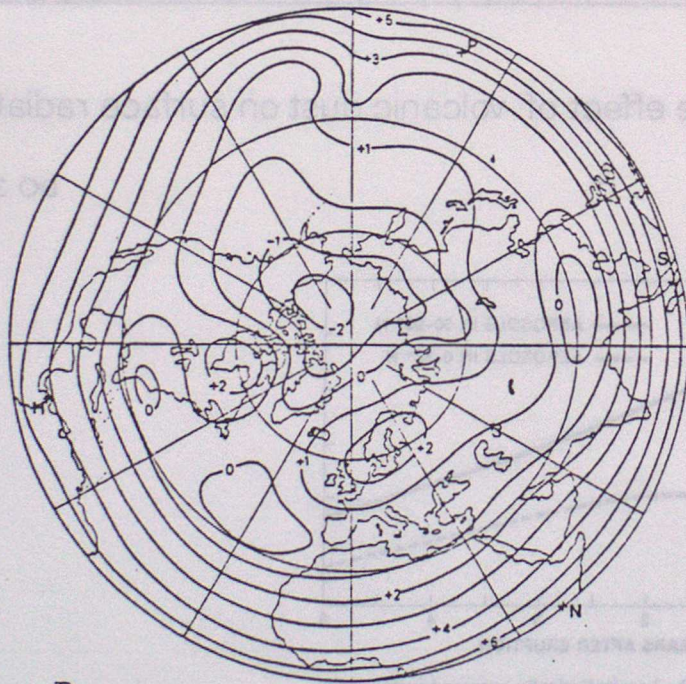
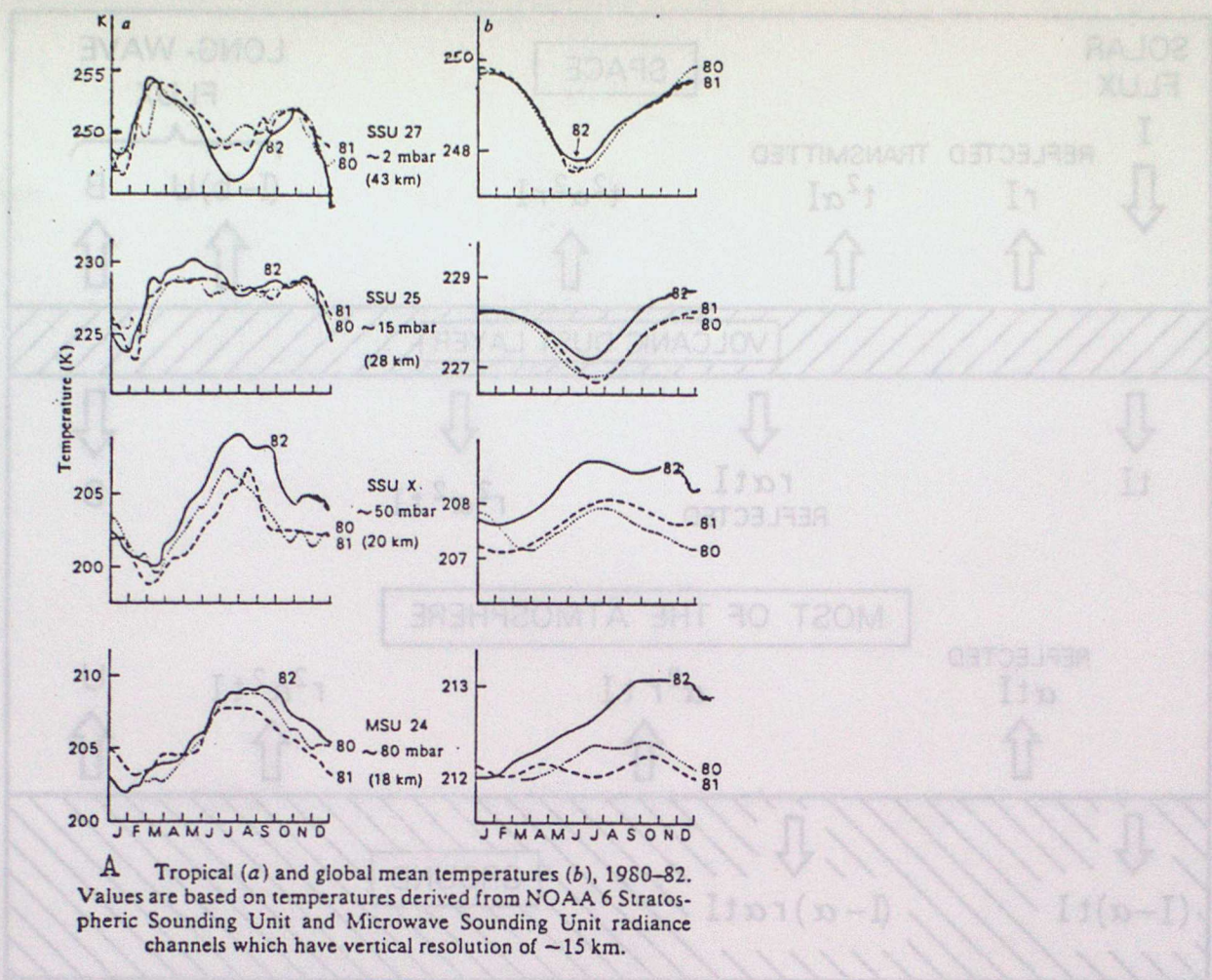


Figure 3.16
 From Robock and Matson
 (1983)

Location of the dust cloud from the El Chichon eruption as observed with visible (VIS) and thermal infrared (TIR) imagery. Portions of the cloud to the right of 180° are plotted at 0000 GMT. Portions to the left of 180° are plotted at 1500 local time. Dash-dot lines indicate difficulties in observing the exact location of the edge of the cloud.



B 30 mbar temperature differences (K) from normal, August 1982. H, Howard Air Force Base; N, Nairobi; P, Ponape; S, Singapore.

Figure 3.17 From Parker and Brownscombe (1983)

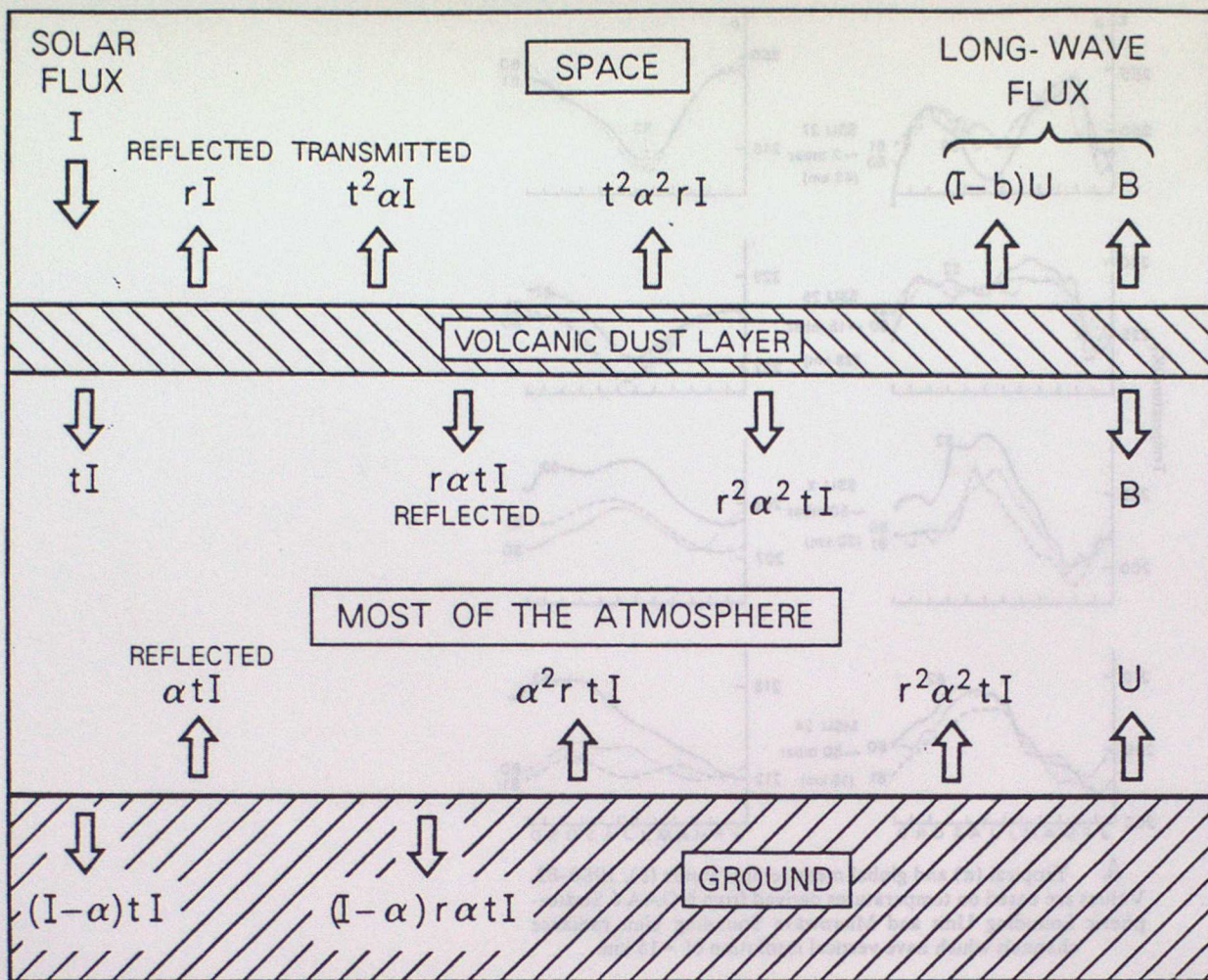
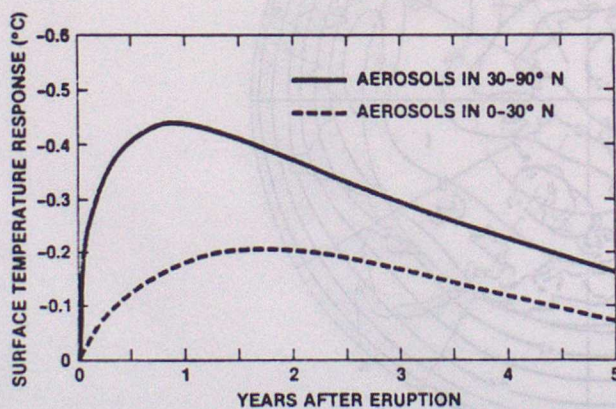


Fig. 3.18 Simple model of the effect of volcanic dust on surface radiation balance.

DO 3723



The response of the hemispherically averaged surface temperature to a uniform distribution of aerosols in the 30-90°N region (solid curve) and in the 0-30°N region (broken curve). The optical thickness of the aerosols is the same as in Fig. 7. of Chou et al (1984)

Figure 3.19 (From Chou et al (1984))

ADVANCED LECTURE NO 4

PART 1 - SOIL MOISTURE AND ALBEDO

4.1 Introduction

In this lecture we consider the possible role of persistent variations of soil moisture and albedo (where the latter are not due to snow - see Appendix 1 to the set of lectures). A general introduction to the problem of the effects of soil moisture and albedo on climate is followed by a selection of results from AGCM experiments which will be referred to again in Lectures 7 and 8.

Charney (1975) wrote a famous paper which contained a simple dynamical model of drought-albedo feedback. This stimulated increased interest in the likelihood of an influence of large-scale anomalies of the albedo of the ground on regional climate fluctuations. Subsequently, it became clear that soil moisture anomalies were just as likely to be important as albedo anomalies but it has long been known that there is a link between the soil moisture of the ground and its albedo. If the ground dries up sufficiently it tends to increase in albedo; albedo is increased further if the vegetation dies back, especially if the drought is long lasting. Charney noted that the Sahara and its overlying atmosphere not only had a high albedo but appeared to be a net radiation sink even in the summer (Fig 4.1).

The 1968-1973 Sahel drought, (which as Lecture 1 mentioned, continued to a new peak of severity in 1984), stimulated Charney to consider whether it might have been partly caused by an increased albedo of the ground which may have been partly man-induced. This could occur through over population, overgrazing by man's animals as well as through the direct effects of drought. Charney considered that if the albedo of dry ground increased, then the radiation available for heating the ground would decrease and this would result in a decline in sensible heating of the atmospheric column above, which should therefore cause the overlying atmosphere to cool. To compensate, large-scale upper convergence followed by sinking motion in the middle troposphere should occur. Sinking would make convection even more difficult and so prolong the drought. One problem with this idea is that if soil moisture before the drought is not zero or there is initially considerable cloudiness and precipitation due to large-scale convergence, then although a small increase in albedo might initiate sinking motion, this would tend to remove some of the existing cloud. Solar heating would increase, offsetting or overcompensating for the effects of the reduced albedo, and perhaps preventing a further increase in sinking motion. In any case there is the distinct possibility that a change of albedo is much less important in prolonging a drought than a deficiency of local soil moisture.

4.1.2 A general discussion of the effect of soil moisture variations on precipitation

Why should we think that soil moisture variations could be important to regional precipitation? Evaporation of water from the ground surface is complex but essentially depends on three factors:-

(a) The difference in vapour pressure between the soil surface and a representative level above the soil; the vapour pressure at the soil surface is usually taken as the saturation vapour pressure of water at the temperature of the soil surface. Thus evaporation depends on ground temperature.

(b) The wind velocity measured at a convenient level near the ground.

(c) The availability of soil water or "soil moisture deficit".

A simple version of Penman's evaporation formula (Penman (1956)) expresses the first two factors:-

$$E_p = 0.35 (e_s - e_a) (0.5 + 0.53v)$$

where e_s equals saturation vapour pressure at the prevailing surface temperature, e_a = average vapour pressure of the air, v = wind speed at a height of 2 m.

E_p is known as the potential evaporation and is nominally the actual evaporation over a flat, fresh-water, surface. However the actual evaporation from a ground surface, E' , is often less than E_p when S , the soil water content, falls below a certain value. Thus a resistance to evaporation builds up as the surface soil layers dry out and the soil water is evaporated from deeper layers. In some AGCM's E' is parameterised as:-

$$E' = \frac{E_p S}{KS_0}$$

Where S = soil water content (the equivalent depth of water in cm existing in the soil), S_0 = the maximum soil water content of the soil or its "field capacity" and K = a constant; $\frac{E_p}{KS_0}$ is sometimes called β .

This formula is a gross oversimplification for vegetated surfaces but does express the most important variations of evaporation rate. For a discussion of evaporation formulae and the water balance of the world, see the authoritative references Baumgartner and Reichel (1975), and Korzun (1978).

4.1.2.1 A schematic demonstration of the importance of soil moisture content to precipitation anomalies

Fig 4.2 shows an idealised picture of the exchange of energy between the ground surface and the atmosphere involving soil moisture and evaporation. Imagine there is no horizontal motion and that cloudiness is fixed. (I am grateful to Dr P Rowntree for the basis of this section). Consider the heat balance of the bottom half of the atmosphere ie that part below 500 mb, which we shall assume to be affected by ground surface processes. The heat balance of the atmosphere can be expressed by:-

$$MC_p \frac{dT}{dt} = H + LP - LE \quad \dots(1)$$

Where E = the evaporation rate, P = the precipitation rate, H = the sensible heating rate, M = the mass of the atmosphere between the surface and 500 mb, per unit area (taken as 1 cm^{-2}), C_p is the specific heat of air and L is its latent heat. In AGCM's (and the real atmosphere) precipitation tends to depend on a relative humidity, $100r$, of about 100% (at some level) being reached. Thus the rate of change of relative humidity of an air mass moving over an evaporating land surface is a crude measure of the time it will take for precipitation to form when convection is important. The rate of change of relative humidity will depend on the soil moisture. We can explore this as follows:-

$$\text{We can write } \frac{dr}{dt} = \frac{d}{dt} \left[\frac{Q}{Q_s} \right]$$

Q = Specific humidity integrated through the column of atmosphere between the surface and 500 mb (above which level moisture content is small)

Q_s = saturation specific humidity in the same column (gm cm^{-2})

$$\text{Thus } \frac{dr}{dt} = \frac{1}{Q_s} \frac{dQ}{dt} - \frac{Q}{Q_s^2} \frac{dQ_s}{dt} \dots (2)$$

$$\text{Now } \frac{dQ}{dt} = E - P \text{ by definition}$$

$$\text{Furthermore } \frac{dQ_s}{dT} = \frac{\delta Q_s}{\delta T} \frac{dT}{dt} \text{ and we can put (approximately)}$$

$$\frac{\delta Q_s}{\delta T} = cQ_s \text{ where } c \text{ is a constant, and } Q = rQ_s.$$

$$\text{So } \frac{dr}{dt} = \frac{E-P}{Q_s} - c r \frac{dT}{dt}$$

From equation (1)

$$\frac{dT}{dt} = \frac{1}{MC_p} [H + L(P - E)]$$

We can put $H + LE = K$, a constant, if the total net rate of heating of the ground due to fixed incident radiation remains constant even though the rate of evaporation may vary due to a reduction in soil moisture. It is easily found that

$$\frac{dr}{dt} = (E - P) \left[\frac{1}{Q_s} + \frac{2cLr}{MC_p} \right] - \frac{cr}{MC_p} (K - LP)$$

$$= (E - P) \left[\frac{1}{Q_s} + \frac{2cLr}{MC_p} \right] - \frac{crK}{MC_p} \text{ if } P \text{ is small } (LP \ll K).$$

The total net heating rate in reasonably sunny conditions in June in S England is approximately the equivalent of 5 mm of evaporation each day ie about $0.5 \text{ g day}^{-1} \text{ cm}^{-2}$. Now $c = 0.07^\circ\text{C}^{-1}$ (approx) from tables (or the Clausius-Clapeyron equation); $L = 2500 \text{ Jg}^{-1}$; $MC_p = 500 \text{ J cm}^{-2} \text{ }^\circ\text{K}^{-1}$ for a 500 mb depth of atmosphere: Q_s is typically about 3 gm cm^{-2} for the lowest 500 mb.

$$\text{If } \frac{Q}{Q_0} = 0.75 \text{ then } \frac{dr}{dt} = 0.86 (E-P) - 0.135 \text{ day}^{-1} \text{ approximately.}$$

$$\text{If } E = 3 \text{ mm/day ie } 0.3 \text{ gm cm}^{-2} \text{ day}^{-1} \text{ and } P = 0 \text{ then } \frac{dr}{dt} = 0.12 \text{ day}^{-1}$$

ie RH increased by $12\% \text{ day}^{-1}$. If $E = 1 \text{ mm/day}$ in drought conditions ie where evaporation is much below the "potential rate", then, still assuming that K remains the same:-

$$\frac{dr}{dt} = -5\% \text{ per day, if } P = 0, \text{ although } K \text{ would change somewhat in reality.}$$

So the likelihood of precipitation is much increased by a wet ground surface. In fact most of the evaporation into a mass of air occurs by day (thus E reaches twice the values indicated above for part of the day); consequently an air mass need only remain over a soil moisture anomaly for about 12 hours for its relative humidity to be effected by the amount calculated. With typical advecting winds of 10 ms^{-1} , the horizontal scale of the soil moisture anomaly need only be about 400-500 km to appreciably affect the humidity of an air-mass moving over it.

4.1.3 Three examples of the sensitivity of climate to albedo (A) and S as shown by AGCM experiments

Mintz (1984) provides a very good summary of 11 AGCM experiments carried out up to 1981. The examples below are chosen to help give a feel for the problem, so they are not always the most elaborate experiments.

4.1.3.1 Experiments with A fixed and different anomaly and control S

(From Shukla and Mintz) (1982)
This experiment used the global GLAS AGCM.

(a) Control - land-surface evaporation was everywhere set at the potential rate E_p (ie where $E = \beta E_p$; β always 1). So the soil was wet everywhere and albedo varied according to a standard climatology. Initial conditions were for the 15 June of a specific year.

- (b) Anomaly - no evaporation was allowed anywhere (dry soil).
Otherwise initial conditions were identical.

The results shown are averages for the following "July". Fig 4.3 shows the precipitation fields for both anomaly and control, Fig 4.4 shows the ground surface temperatures and Fig 4.5 the PMSL fields. Precipitation is greatly reduced over most of the continents in the anomaly experiment except near the ITCZ and in parts of Asia, though Sahel rainfall, itself a product of the ITCZ, is also reduced in this experiment. Furthermore, in the anomaly experiment, there is some reduction of overall precipitation over the oceans. The most dramatic effect of stopping evaporation over land in the summer half of the world and in the tropics is to greatly increase the surface temperature of the ground. Part of this increase in temperature is due to the resulting decreased cloudiness as is shown by Fig 4.6; here R_s , the solar heating rate, increases due to cloudiness and less latent heating. Not surprisingly, long-wave radiation losses from the ground are larger and of course the sensible heating vastly increases. Fig 4.5 shows that, on the whole, pressure falls over the continents and rises over the oceans, giving a strong global monsoon circulation component to the anomalous atmospheric response. No estimates of statistical significance are given but a qualitative response of the kind shown is physically reasonable and is shown in other similar AGCM experiments, even where experimental design is more complex. Of course the computed changes in evaporation are unrealistically large. (See the results of a more realistic experiment in Lecture 8).

4.1.3.2 Different values of A but fixed values of S

(Charney et al) (1977)

Here we look at a restricted but interesting aspect of Charney et al's results; the Sahel drought is a theme of these lectures, so we will look at the energy balance over the Sahel when A is changed.

(a) Control - where the continents are ice and snow free they are given an albedo of 0.14 though where true deserts are observed, the albedo is set to 0.35 (Fig 4.7).

(b) Anomaly - same conditions except that the albedo is increased from 0.14 to 0.35 in the "Sahel", in Rajputana (India) and also in the Western Great Plains (USA), all adjacent to true deserts (see Fig 4.7). Table 4.1 shows detailed results for the energy balance of the Sahel which are instructive, given Charney's original paper of 1975. The main points are:

(1) The evaporation rate, βE_p , is fixed at 0.51 E_p in both experiments.

(2) The solar heating rate of the ground, R_s , increases slightly as A increases; this paradoxical result arises because the model cloudiness, N, decreases greatly from 0.7 to 0.46, more than necessary to offset the effects of an increased value of A.

(3) Evaporation decreases in the anomaly experiment, though only by 1 mm/day.

- (4) Sensible heating increases in the anomaly experiment.
- (5) In the anomaly experiment long-wave radiation increases due to clearer skies and less humid air.
- (6) Net radiation, R_n , becomes less positive.
- (7) Surface temperature falls in the anomaly experiments but only very slightly. (T_a).
- (8) The convergence of water vapour in the anomaly experiment decreases very strongly, by the equivalent of 2.5 mm of precipitation per day.
- (9) Precipitation is considerably reduced in the anomaly experiment (by 3.4 mm per day) - mostly because of the decreased moisture convergence rather than because of the decreased evaporation.

So the dynamical effect of decreased convergence from more distant locations is dominant when A is increased, but surface temperatures hardly alter, even though the availability of soil moisture is fixed (as effectively assumed in Charney's original model). Such results clearly depend on the model used but show the fascinating complexity of the problem. They do not prove however that an increase in albedo is necessarily the chief (local) cause of the Sahel drought as the next section will suggest.

4.1.3.3 Fixed A, but different time-dependent soil moisture variations - West Africa only

(Walker and Rowntree) (1977)

The model used was a restricted area 11-level AGCM. Because of this, it may not properly represent changes in large scale moisture convergence. Nevertheless the experiment is instructive as soil moisture was allowed to vary through the experiments as P and E varied.

1. Case 1 - initial S = 0 in the latitudes 14-32°N; initial S = 100 mm in zones 6-14°N and 32-36°N

Case 2 - initial S = 100 mm over all land regions.

In this model, $\beta = 1$ when S is greater than or equal to 50 mm and the maximum S = 150 mm (run off immediately occurs for greater values). Fig 4.8 shows the variation of precipitation and soil moisture for days 1-10 (case 1 experiment) and similar maps for days 1-20 (case 2 experiment). In case 1, where the soil was initially dry, it remains dry. There is very little water transport into the dry region and practically no precipitation. The wetter soil regions to the south of 14°N have a variable precipitation rate as wave-like model disturbances move across these regions; however total precipitation is quite considerable. In case 2, the initially moist Sahara rapidly develops rainfall which persists. The Saharan soil moisture at first declines but steadies after 10 days. Coastal precipitation and soil moisture vary markedly on short timescales due to

transient wave disturbances but precipitation is quite high. Although the integrations were very short, this simple model appeared to give two solutions to the Sahara/Sahel climate that looked distinctly "intransitive", though strong seasonal variations in circulation in this region would make this an unlikely possibility in the real atmosphere. Despite the simplicity of the model it shows that a Sahel drought, in a given season, could easily be made worse by changes in circulation that initially tend to reduce the soil moisture which might then provide a powerful feedback on the rainfall. Changes in albedo may not be necessary (and have probably been modest over the Sahel region in the last 15 years).

Summary

4.1.4 The results of this section suggest that soil moisture, especially, may provide a new source of potential predictability on the stream 1 (1-3 months) and possibly stream 2 timescales of the World Climate Research Programme.

REFERENCES TO LECTURE 4 PART I

BAUMGARTNER A AND REICHEL E (1975) The World Water Balance: Mean annual global, continental and maritime precipitation, evaporation and run-off. Elsevier.

CHARNEY, J G (1975) Dynamics of deserts and drought in the Sahel. Q J Roy Met Soc, 101, pp 193-202.

CHARNEY J, QUIRK W J, CHOW S-H AND KORNFIELD J (1977) A comparative study of the effects of albedo change and drought in semi-arid regions. J Atmos Sci, 34, pp 1366-1385.

KORZUN V I (Ed) (1978) World Water balance and water resources of Earth. Studies and Reports in Hydrology, Vol 25, Unesco Press, Paris.

MINTZ Y (1984) The sensitivity of numerically simulated climates to land-surface boundary conditions. The Global Climate, pp 79-105. Ed: J T Houghton, Cambridge University Press.

PENMAN H L (1956) Estimating Evaporation. Trans Amer Geophys Union, 37(1), pp 43-46.

SHUKLA J AND MINTZ Y (1982) Influence of land-surface evapotranspiration on the earth's climate. Science, 215, pp 1498-1501. Also presented at the JSC Study Conference on Land Surface processes in atmospheric general circulation models, Greenbelt, USA, 5-10 January 1981 (this is reference on diagrams).

WALKER J AND ROWNTREE P R (1977) The effect of soil moisture on circulation and rainfall in a tropical model. Q J Roy Met Soc, 103, pp 29-46.

ADVANCED LECTURE NO 4

PART II - SEA SURFACE TEMPERATURE (SST)

4.2.1 Introduction

SST varies quite substantially through the seasons in many regions and it is well-known that differences in temperature between land and sea play an important role in shaping the observed seasonal variations in atmospheric circulation. Fig 4.9 shows the mean range of air temperature and SST over the globe between the coldest and warmest months. It is not, at first sight, completely obvious that variations in SST that occur in addition to the mean seasonal variations could be important in climate variability. In this lecture we concentrate mainly on the effects of SST anomalies on the 1-2 month timescales with an eye to the long range forecasting problem. We leave discussion of longer timescales (with one exception) to Lectures 5 and 8. Lecture 5 will discuss the El Nino - Southern Oscillation (ENSO) phenomenon so little mention of ENSO will be made here.

4.2.2 What size of SST anomaly is important?

The discussion below is reminiscent of that presented by Sawyer (1965). At the most elementary level, imagine the temperature of the air to be increased over a large area by 1°C throughout the depth of the troposphere (up to say 200 mb) with no change elsewhere. If there was no immediate dynamically induced response from the surrounding atmosphere other than to accept an inflow at higher levels of excess warm air, the density of the warm air, using Boyle's law, would fall by roughly $1/T$ where T is the air temperature, ie by roughly $1/300$. So PMSL would fall by approximately 0.8 ($1000-200/300$) mb or about 3 mb. To be effective in altering large scale circulation, in middle latitudes, we could imagine that the horizontal scales of the SST anomaly might have to exceed about $1/4$ of a typical Rossby wave length - say 1000 km. The anomalous rate of heat transfer (reckoned as positive when into the ocean) that would initially occur if the SST anomaly was suddenly "switched on" is given adequately by the sum of the anomalous sensible and latent heating that would be produced:-

$$\begin{aligned} \text{ie } \Delta Q &= \Delta H + \Delta E \\ &= 3.7 U \Delta (e_a - e_s) + 2.4 U \Delta (T_a - T_s) \quad \text{Wm}^{-2} \end{aligned}$$

from standard formulae. e_a = vapour pressure of the air (mb), e_s is the saturation vapour pressure at the sea temperature, U = wind speed in ms^{-1} .

If we assume that the initial relative humidity = 80% and $T = 15^\circ\text{C}$ and that it is mid-latitude winter with $U = 10 \text{ ms}^{-1}$ then we find $\Delta Q = 70 \text{ Wm}^{-2}$ approximately when T_s changes by 1°C. Although this calculation somewhat exaggerates ΔQ because e_a and T_a are held fixed, this amount is about 30% of the effective annual mean solar insolation warming the mid-latitude ocean (about 250 Wm^{-2}), suggesting that a reasonably large scale winter mid-latitude SST anomaly of 1°C might be significant in regions of strong winds and strong cold advection. In summer, when mean wind speeds are typically half their winter values, the anomalous heat transfer would (approximately) also be halved. Fig 4.10 shows the annual average heat flux, including net radiation, from the Atlantic Ocean to the overlying atmosphere, given that the sign of the values shown is reversed. Near the

ITCZ, heat is transferred from the ocean to the atmosphere by deep convection. A similar analysis shows that for SST of 29.5°C (the average value in the warmest tropical regions) an increase of SST by 1°C would produce a similar anomalous heat transfer when the mean wind speed was only 5 ms⁻¹, a typical value. This anomalous amount is comparable to the average heat transfer in tropical regions. It is difficult to determine the areal size of the anomaly that will be significant however. So anomalies of 1°C or more that last say 2 months or so and cover at least 1 x 10⁶ km² could significantly affect sequences of circulations "regimes" in a number of regions.

4.2.3 What SST anomaly (SSTA) variations actually occur?

Fig 4.11(a) (b) show the standard deviation of January and July SST derived from MOHSST (Version 3) for the period 1951-80. Areas of high inter-annual variability include the tropical, Central and East Pacific, the Central Pacific and the Kuroshio and Gulf Stream regions. Fig 4.12 gives a rather better measure of the persistence of SSTA and shows areas of the world where a 1°C 10° x 10° anomaly (a) occurs and (b) on average persists (taking all calendar months together) for two months or more:-

- (a) The tropical C and E Pacific
- (b) The Eastern, Northern and Northwestern extratropical Pacific.
- (c) The South east Tropical S Atlantic
- (d) Several parts of the western Indian Ocean
- (e) The tropical Central N Atlantic
- (f) The North West Extratropical Atlantic
- (g) Isolated areas of the Extratropical S Pacific, most notably west of Chile, though analyses are not very reliable here.

Further analyses show that although the Tropical W Pacific generally exhibits small anomalies, they are likely to be particularly persistent. The above information is taken from Newman and Storey (1985).

4.2.4 Effects of Extra Tropical SSTs on atmospheric circulation

Smagorinsky (1953) carried out the first physically realistic analysis, using a baroclinic model, of the perturbations in the extratropics of a zonally symmetric wind flow by imposed diabatic heating rates (on large space scales) that varied along latitude circles. Fig 4.13 is representative of his results. Smagorinsky defined a sinusoidal heating function so that in Fig 4.13 the maximum diabatic heating, Q_{max} , was 209 Wm⁻² relative to the minimum heating, Q_{min} . The wavelength of the heating function was 160° and in Fig 4.13 the maximum heating is placed at 40° relative longitude and the minimum heating at -40°. Smagorinsky designed the wavelength of this heating variation to correspond roughly with the variation in surface heating in winter due to the distribution of land and sea in the N American sector. He showed (which can be deduced from Fig 4.13) that the Iceland low at the surface should be placed about 20-30°

longitude East of the 500 mb Canadian trough in the winter. In Fig 4.13, D is the meridional wavelength of the heating, h is the height of maximum heating (which includes the effects of latent heat release): for our purpose $D = 35^\circ$ is quite appropriate (Fig 4.13(a),(b)). This value corresponds to an appreciable positive (or negative) heating anomaly that occupies at least 10° of latitude. Fig 4.13 suggests that the maximum PMSL response would be of magnitude $1 \text{ mb}/20 \text{ MW cm}^{-2}$ of forcing and the maximum 500 mb height response would be about $1 \text{ dm}/30 \text{ MW cm}^{-2}$.

We can attempt to apply these ideas to work carried out by Ratcliffe and Murray (1970) (RM) who showed from observations an association between N Hemisphere PMSL anomalies and SSTA in the previous month south east of Newfoundland. Fig 4.14 shows the SSTA pattern, in a generalised way, and Fig 4.15(a), (b) the response of the PMSL to warm and cool anomalies; their pattern is reminiscent of Smagorinsky's results. Concentrating on February PMSL response, the magnitude of the PMSL anomalies is roughly the same for both cool and warm SSTA though the patterns are not the inverse of each other, suggesting analysis difficulties or non-linearity in the response of PMSL to SSTA. Nevertheless in February, U is approximately 12 m sec^{-1} south east of Newfoundland, $T_s =$ approximately 10°C so a mean maximum SSTA of 1.5°C might give a maximum heating anomaly of about $80\text{-}90 \text{ Wm}^{-2}$. Fig 4.13 suggests a PMSL response downstream of this SSTA value of about 4 mbar, quite similar to RM's value for positive SSTA, though the observed PMSL anomaly for cold SSTA is rather displaced from its expected position suggesting that Smagorinsky's model is not wholly appropriate for a relatively small areal SST anomaly size. In summer the general shape of the PMSL anomaly pattern is similar but anomalies are about half those observed in February. This seems reasonable as on average U will be about half the value observed in February.

Recently, RM's results have been tested in winter by Palmer and Sun (PS) using the Meteorological Office 5-level AGCM supported by an observational analysis employing better SST data than was available to RM (from the MOHSST (Version 3) data set). The modelling study used warm and cold SSTA whose maximum magnitude just exceeded 3°C ie double that used by RM; these anomalies are still realistic and correspond to the maximum observed anomalies. The model was initialised from real November atmospheric data and used winter radiation. Four pairs of anomaly (warm SST) and control (cold SSTA) runs were made. December climatological mean SST was used away from the anomaly. The difference in model 1000 mb height and 500 mb height is shown in Fig 4.16 (a)-(b); in each diagram the difference is averaged over the four pairs of integrations for model days 21-50. The patterns are reminiscent of those of RM but the (statistically significant) high and low centres are further apart. Other details of the model response are given in the paper including the anomalous tracks of depressions. PS believe that the anomalous advection of low-level warm, humid air into the anomaly area from the south is an important component of the atmospheric response, which also tends to maintain the SST anomaly. This provides an important difference between the Smagorinsky model and the probable atmospheric response over the "Ratcliffe" area.

The observational study consisted of a calculation of PMSL and 500 mbar height differences between winter months (Nov-Feb) having a warm SSTA ($>$ about 0.9°C) and those having a cool SSTA ($<$ about 0.9°C) in the region $40^\circ\text{-}60^\circ\text{W}$, $40^\circ\text{-}50^\circ\text{N}$. The epoch 1951-80 was studied first and gave similar

results to those of the AGCM though with a slightly shorter wavelength between high and low centres at both levels, when monthly mean SSTA, PMSL and 500 mb height were calculated for the same month. The analysis was repeated for 1901-30 and gave similar results. Fig 4.17 is an example of results for 1951-80. However a puzzling and as yet unresolved result was that when PMSL was allowed to lag one month behind SSTA the relationships did not hold up well nor did they agree well with those of RM - low pressure anomalies were indicated stretching across the Atlantic when months following warm SSTA were subtracted from those following cold SSTA.

Rowntree (1984) has summarised a number of AGCM experiments carried out in the Atlantic and Pacific on mid-latitude SSTA; Fig 4.18 shows his summary diagrammatically; the overall conclusions are surprisingly consistent and broadly in harmony with the ideas of Smagorinsky, though in reality, as hinted above, the relative importance of different physical effects in the atmosphere may vary considerably. Rowntree (1979) provides another useful review of AGCM extratropical SST forcing experiments; Maryon (1981) provides a detailed review of observational studies and some AGCM studies of extra-tropical and tropical SSTA - atmospheric forcing (or empirical associations).

4.2.5 Tropical SSTA

The nature of atmospheric forcing by Tropical SSTA forcing is different. Typically, warm tropical waters are associated with a low level tropospheric (pressure) trough and an overlying upper tropospheric (pressure) ridge. Anomalous tropical heating mainly gives rise to anomalous near vertical atmospheric motion. So the most direct result of warm tropical SSTA forcing is that an anomalous warm upper high is forced near the SSTA anomaly, ie anomalous high-level anticyclonic vorticity is created. Simmons (1982) has, amongst others, used a relatively simple baroclinic model to show that the resulting anomalous atmospheric vorticity forcing gives rise to a Rossby wave-like response in the extratropics; this is associated with the stimulation of barotropic instability in the climatological mean upper flow (initially prescribed in Simmons' model). The atmospheric response in the winter is largest when the vorticity forcing is placed in specific tropical longitudes, i.e. the climatological mean upper flow, including its mean troughs and ridges, is initially prescribed. This longitudinally varying response does not occur for a prescribed zonally averaged mean flow. Simmons suggests that the effects of tropical vorticity forcing propagate into mid latitudes more easily when the forcing is overlain by upper westerly winds. For upper level anticyclonic vorticity forcing, such propagation is favoured when the forcing coincides with a climatological upper ridge as in the tropical W Pacific in winter. Fig 4.19 shows a few of Simmons' results at 500 mb using a January mean 500 mb height climatology where vorticity is forced in different tropical regions (SST forcing was not explicitly used). Fig 4.19 shows that the strongest extratropical response that Simmons found was for forcing centred at 15°N, 135°E. Notice that the 500 mb height response is quite large near UK (in the model).

Palmer and Mansfield (PM) (1985) have used the Meteorological Office 11-level AGCM to explore the impact of tropical W Pacific SSTA on winter atmospheric circulation. They found that an anomaly with a maximum of just over 1°C centred on the equator in the tropical W Pacific (see Fig 4.20(a))

produces a strong wave-like response at 500 mb (Fig 4.20(b)). The response is qualitatively similar to that of Simmons though the path of PM's 500 mb height anomalies across polar regions is appreciably different. In a companion paper, (Palmer (1985)), it is argued that the atmospheric response to tropical vorticity forcing may be non-linear; vorticity forcing from positive SSTA anomalies mainly results from the increased release of latent heat which appears to increase non-linearly with increasing SSTA. So it might be expected that a negative SSTA of given magnitude would produce a smaller vorticity forcing and atmospheric response. Palmer has provided evidence for a similar magnitude of atmospheric response, though of opposite sign, and gives a straightforward dynamical explanation. However it remains to be seen to what extent such results depend on the AGCM used. A contributory reason for the very strong atmospheric response to anomalies of SSTA over the W Pacific is that a given SSTA produces a large anomaly of latent heating than elsewhere; the saturation vapour pressure of ocean water changes considerably faster as temperature changes in the very warm W Pacific water than it does in middle latitudes. Typical tropical W Pacific SST's exceed 29°C; at the time of writing (mid-February 1985), SST maxima exceed 31°C quite close to the position of the maximum tropical W Pacific SST anomaly used by PM.

Fig 4.21 shows the response of a steady state linear model (from Simmons (1982)) to an isolated positive diabatic heating anomaly near the equator. To the west of the heating maximum, the low level winds tend to be westerly and the upper level winds easterly, a similar situation to that in the real atmosphere west of the diabatic heating maximum created by the SE Asian monsoon/W Pacific region in northern summer (see Lecture 2). To the east of the heating maximum, the model winds are reversed: ie the upper winds are westerly and the lower winds easterly. Sinking motion should occur over the well-defined SST minimum near the equatorial S American coast and connect the mean upper westerly to the mean lower easterly flows that exist to the east of the W Pacific SST maximum. The closed circulation that results is like the Walker circulation discussed in Lecture 2: the mechanism underlying Fig 4.21 probably explains an appreciable part of the Pacific Walker circulation and, perhaps, similar circulations near the equator in other longitudes.

Rowntree (1976) carried out experiments using the Met Office 5-level AGCM which indicated, in winter, that north of a positive SST anomaly placed in the tropical NE Atlantic a surface low was formed, with an upper high almost over the anomaly. North of the low, but well into middle latitudes and longitudes, a high anomaly was found. Fig 4.22 shows the model response for selected experiments compared to control integrations. The SST anomaly was based on that observed at the beginning of the very cold European winter of 1962-3 but it remains unclear to what extent Rowntree's results "explain" that winter. Figs 4.22b and c give a slightly different response because of small changes in model formulation and indicate the sensitivity of the results to such small changes. This is clearly not enough to change the nature of the response in a fundamental way but Figs 4.22b and c highlight one of the problems in interpreting the results of model integrations, a problem still evident with current models.

Hastenrath (1984) has also carried out interesting observational studies of tropical Atlantic SSTA and circulation anomalies near NE Brazil to try to provide a partial explanation of recurring droughts in that region.

4.2.6 Another way in which SSTA can influence climate

SSTA can affect climate in maritime regions by directly cooling or warming the overlying air and thus the downwind land air. Consider a fixed atmospheric circulation pattern: Parker (1984) has shown a very interesting correlation between decadal averages of temperature observed in Central England during Lamb "westerly" circulation types (see Lamb (1972b) and Lecture 1 for discussion of Lamb types) and decadal averages of SST calculated over the whole N Atlantic north of 35°N (Fig 4.23). Their correlation was 0.67 for the decades 1861-1870 to 1971-1980. Although this correlation could arise from the influence of a third factor, the relationship is physically reasonable because SST has varied in a similar way over most of the N Atlantic on these time scales (Folland, Newman and Parker, unpublished work). SSTA vary by larger amplitudes on shorter time scales; so turning to a moment to the long-range forecast problem, it seems worthwhile investigating, for suitable fixed air masses and seasons of the year, relationships between regional air temperature anomalies over UK and SSTA in the surrounding seas.

REFERENCES TO LECTURE 4 PART II

- BUNKER, A F (1980) Trends of variables and energy fluxes over the Atlantic Ocean from 1948 to 1972. *Mon Weath Rev*, 108, pp 720-732.
- FOLLAND, C K (1983) Regional-scale interannual variability of climate - a north west European perspective. *Met Mag*, 112, pp 163-183.
- FOLLAND, C K, PARKER, D E AND KATES, F E (1984) Worldwide marine temperature fluctuations 1856-1981, *Nature*, 310, pp 670-673.
- HASTENRATH, S (1984) Interannual variability and annual cycle: Mechanisms of circulation and climate in the tropical Atlantic sector. *Mon Weath Rev*, 112, pp 1097-1107.
- LAMB, H H (1972a) *Climate Present, Past and Future*, Vol 1. Methuen.
- LAMB, H H (1972b) British isles weather types and a register of the daily sequence of circulation patterns 1861-1971. *Met Office Geophys Mem Vol XVI No 116*, HMSO, London.
- MARYON, R H (1981) A review of recent studies into the forcing of the atmospheric circulation by sea-surface temperature anomalies. *Met O 13 Branch Memo No 116*.
- MONIN, A S (1975) The role of the oceans in climatic models. *ICSU/WMO, GARP Publ Ser No 16*, Geneva, pp 201-205.
- NEWMAN, M R AND STOREY, A M (1985) A preliminary study of intermonthly changes in sea surface temperature anomalies throughout the world ocean. *Coupled ocean-atmosphere models*, pp 391-404. Ed: J Nihoul, Elsevier.
- PALMER, T N (1985) Response of the UK Met Office general circulation model to sea surface temperature anomalies in the Tropical Pacific Ocean. *Coupled Ocean-Atmosphere Models*, pp 83-106. Ed: J Nihoul, Elsevier.
- PALMER, T N AND MANSFIELD, D A (1984) Response of two atmospheric general circulation models to sea-surface temperature anomalies in the tropical East and West Pacific. *Nature*, 310, pp 483-485.
- PALMER, T N AND SUN-Z (1985) A modelling and observational study of the relationship between sea surface temperature in the North West Atlantic and the atmospheric general circulation. *Q J Roy Met Soc*, (in Press).
- PARKER, D E (1984) *Met O 13 Discussion Note No 81*.
- RATCLIFFE, R A S AND MURRAY, R (1970) New lag associations between N Atlantic sea temperature and European pressure applied to long-range weather forecasting. *Q J Roy Met Soc*, 96, pp 226-246.
- ROWNTREE, P R (1976) Response to the atmosphere to a tropical Atlantic ocean temperature anomaly. *Q J Roy Met Soc*, 102, pp 607-626.
- ROWNTREE, P R (1979) The effects of changes in ocean temperature on the atmosphere. *Dynamics of Atmospheres and Oceans*, 3, pp 373-390.

ROWNTREE, P R (1984) A survey of ocean surface temperature anomaly experiments for the N Hemisphere winter. Met O 20 Technical Note II/220.

SAWYER, J S (1965) Notes on the possible physical causes of long-term weather anomalies. WMO Tech Note, No 66, pp 227-48, Geneva.

SIMMONS, A J (1982) The forcing of stationary wave motion by tropical diabatic heating. Q J Roy Met Soc, 108, pp 503-534.

SMAGORINSKY, J (1953) The dynamical influence of large-scale heat sources and sinks on the quasi-stationary mean motions of the atmosphere. Q J Roy Met Soc, 79, pp 342-366.

LAMB, H H (1972a) Climate Present, Past and Future, Vol 1. Methuen.

LAMB, H H (1972b) British Isles weather types and a register of the daily dependence of circulation patterns 1861-1971. Met Office Geophys Mem No 121. No 116, HMSO, London.

MARION, S H (1981) A review of recent studies into the forcing of the atmospheric circulation by sea-surface temperature anomalies. Met O 13 Discussion Note No 118.

MONTM, A S (1975) The role of the oceans in climatic models. ICSU/WHO, GARP Publ Ser No 16, Geneva, pp 201-205.

NEWMAN, M R AND STORCY, A M (1985) A preliminary study of interannual changes in sea surface temperature anomalies throughout the world ocean. Coupled Ocean-Atmosphere Models, pp 301-404. Ed: J Nichol, Elsevier.

PALMER, T N (1985) Response of the UK Met Office general circulation model to sea surface temperature anomalies in the tropical Pacific Ocean. Coupled Ocean-Atmosphere Models, pp 83-106. Ed: J Nichol, Elsevier.

PALMER, T N AND MARSHFIELD, D A (1984) Response of two atmospheric general circulation models to sea-surface temperature anomalies in the tropical East and West Pacific. Nature, 310, pp 483-485.

PALMER, T N AND BUN-2 (1985) A modelling and observational study of the relationship between sea surface temperature in the North West Atlantic and the atmospheric general circulation. Q J Roy Met Soc, (in press).

PARKER, D E (1984) Met O 13 Discussion Note No 81.

HATCLIFFE, R A S AND HURRAY, R (1970) Sea lag associations between N Atlantic sea temperature and European pressure applied to long-range weather forecasting. Q J Roy Met Soc, 96, pp 126-144.

ROWNTREE, P R (1976) Response to the atmosphere to a tropical Atlantic ocean temperature anomaly. Q J Roy Met Soc, 102, pp 607-628.

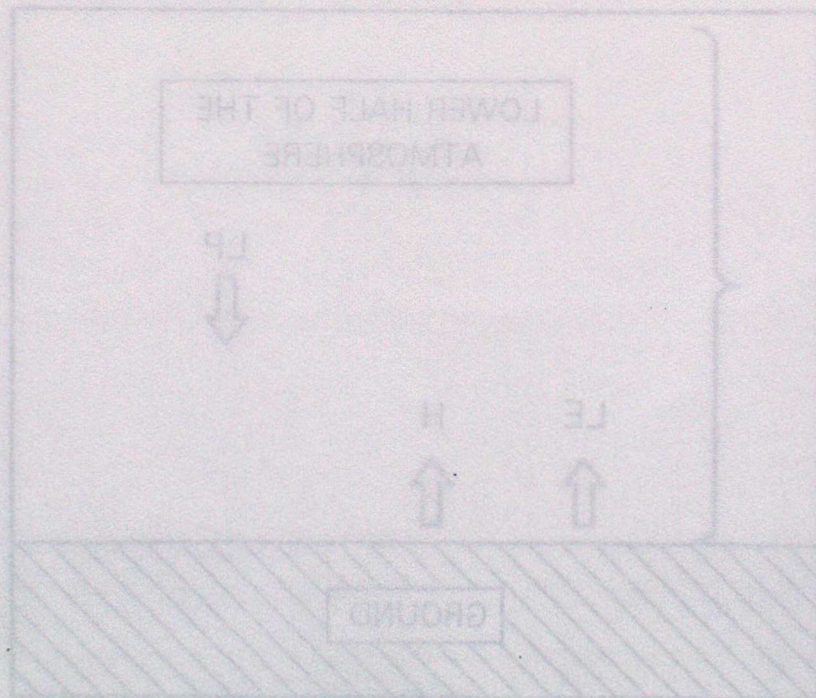
ROWNTREE, P R (1979) The effects of changes in ocean temperature on the atmosphere. Dynamics of Atmospheres and Oceans, 2, pp 373-398.

Energy balance

Water balance

Region	Case No.	Energy balance					Water balance						
		(1) β	(2) $(1-\alpha)$	(3) R_S	(4) R_L	(5) R_N	(6) LE	(7) H	(8) N	(9) T_A	(10) E	(11) $(-\nabla \cdot q_v)$	(12) P
Sahel (16°-20°N 17.5°W-37.5°E)	2a	0.51	0.86	169	58	111	107	4	0.70	26.0	3.7	3.7	7.4
	3a	0.51	0.65	177	84	93	81	12	0.46	25.7	2.8	1.2	4.0

Table 4.1 Components of the energy and water budgets, in experiment of Charney et al (1977)



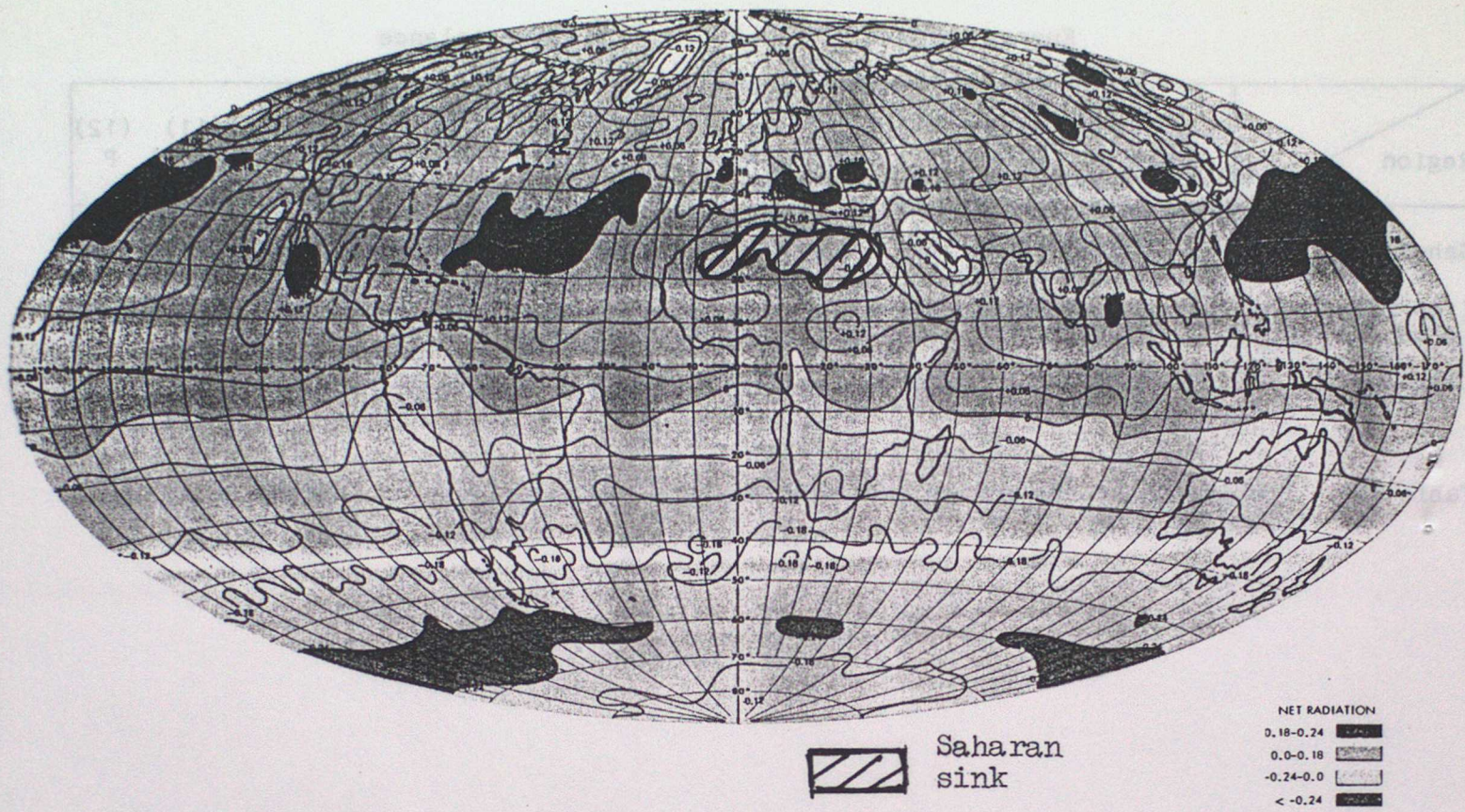


Figure 4.1 Net radiation at the top of the atmosphere (cal/cm²/min) measured from Nimbus III, 1-15 July 1969. From Charney (1975)

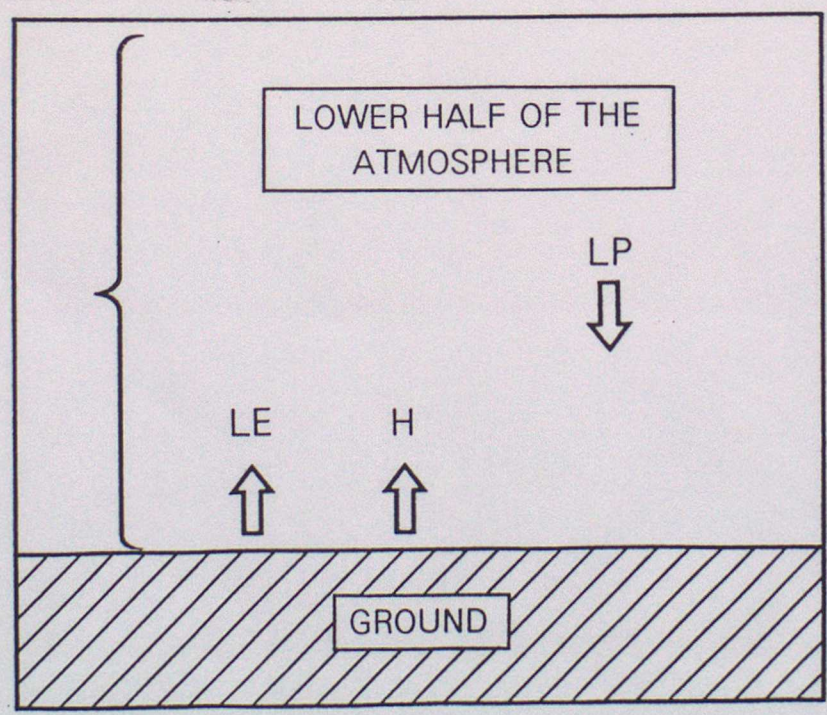


Fig. 4.2 Precipitation and soil moisture anomalies

Precipitation (mm/day) in wet-soil case (top) and dry-soil case (bottom), in experiment of Shukla & Mintz (1981). (Precipitation greater than 2 mm/day is shaded.)

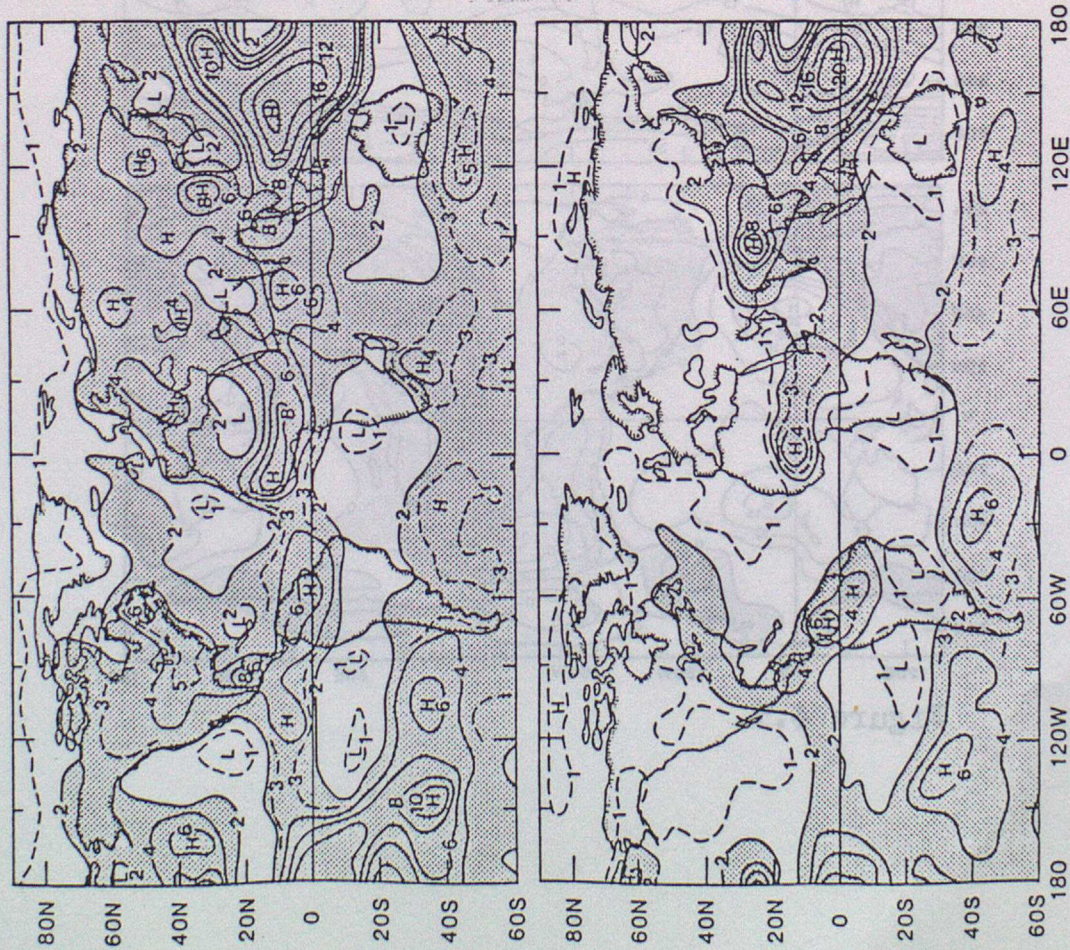


Figure 4.3

Ground-surface temperature (°C) in wet-soil case (top) and dry-soil case (bottom), in experiment of Shukla & Mintz (1981).

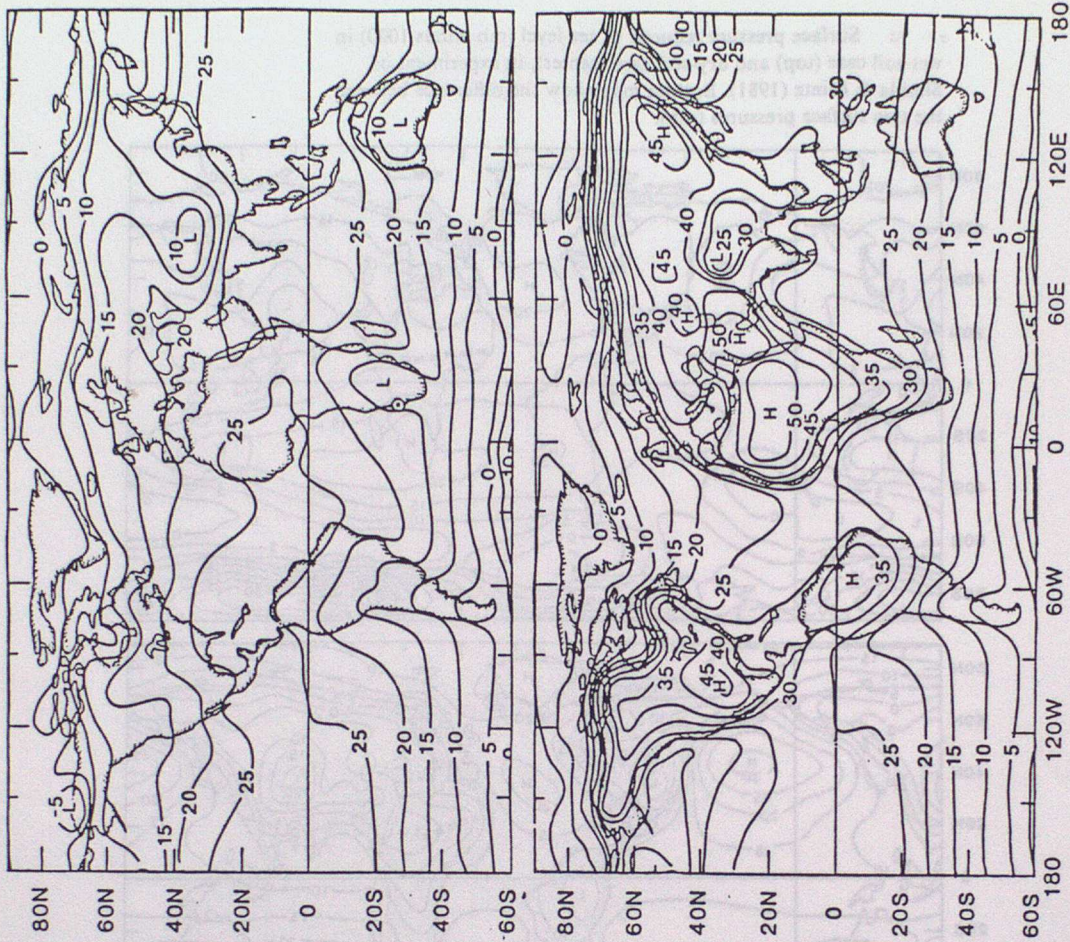


Figure 4.4

Surface pressure reduced to sea level (mb minus 1000) in wet-soil case (top) and dry-soil case (center), in experiment of Shukla & Mintz (1981). Bottom map show the difference between the two surface pressures (mb).

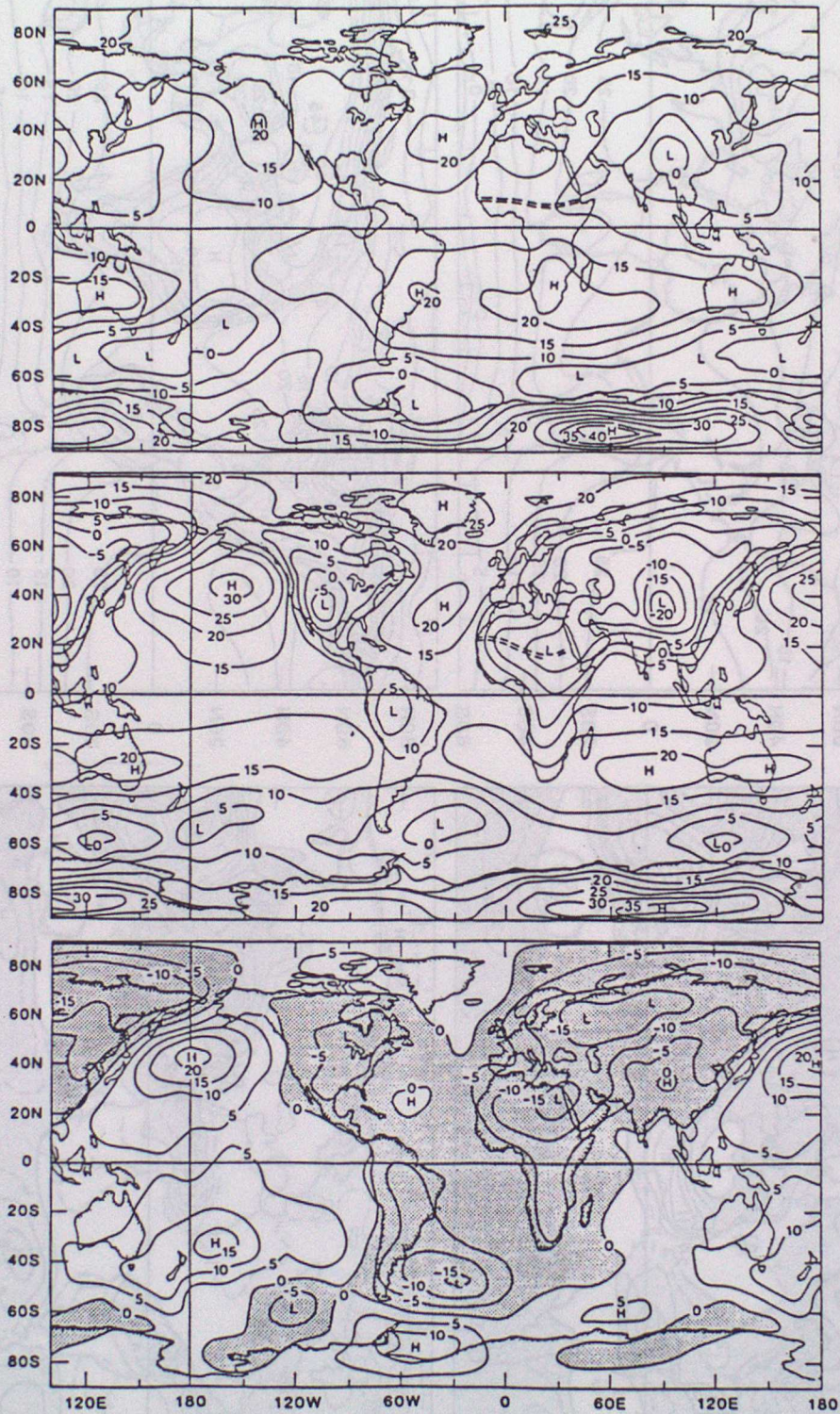


Figure 4.5

Surface energy transfers (watt/m²) averaged for the continents between 20°S and 60°N, in experiment of Shukla and Mintz (1981).

- R_s solar radiational heating of the ground.
- R_L long wave radiational cooling of the ground (difference between radiation emitted by ground and radiation absorbed by ground).
- $R_N = (R_s - R_L)$ net (all-wavelength) radiational heating of the ground.
- LE latent heat transfer from ground to atmosphere (evaporative cooling of the ground).
- H conductive-convective heat transfer from ground to atmosphere.

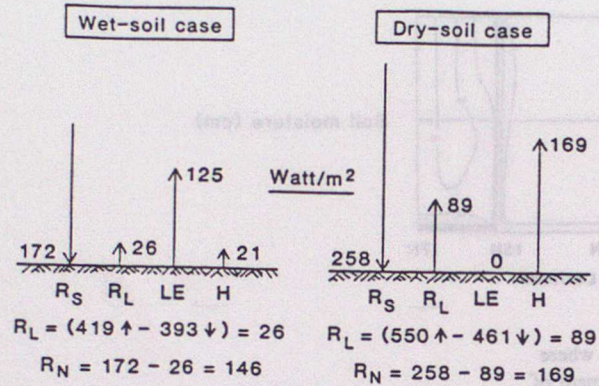


Figure 4.6

Bottom panel: the assigned albedos in experiments of Charney *et al.* (1977). Unshaded land areas have an albedo of 0.14 in all cases, and dot-shaded areas have an albedo of 0.35 in all cases. In the cross-ruled areas the albedo was changed from 0.14 (in cases 2a and 2b) to 0.35 (in cases 3a and 3b). Top panel: precipitation (mm/day) in case 3b.

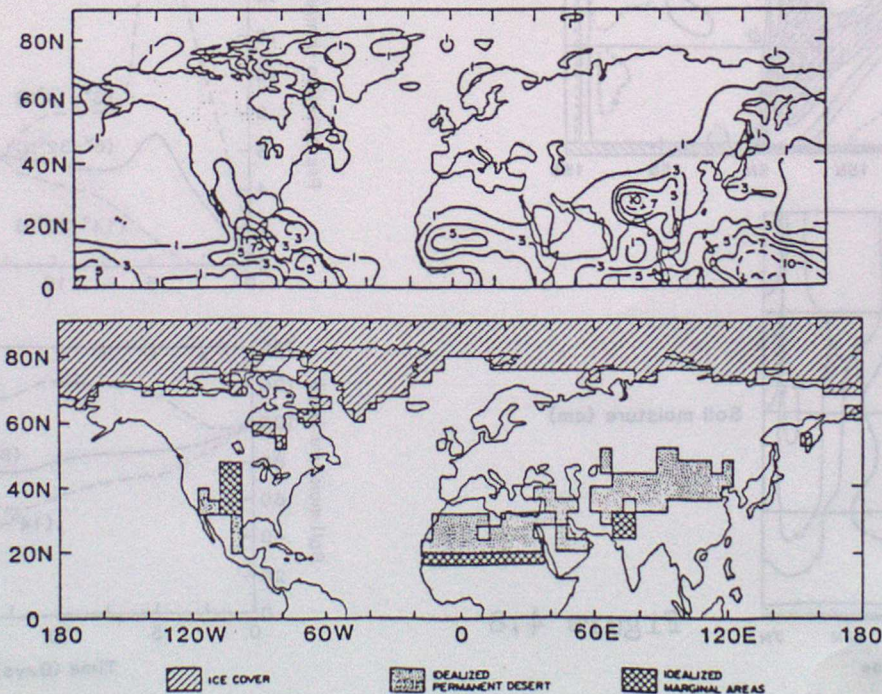
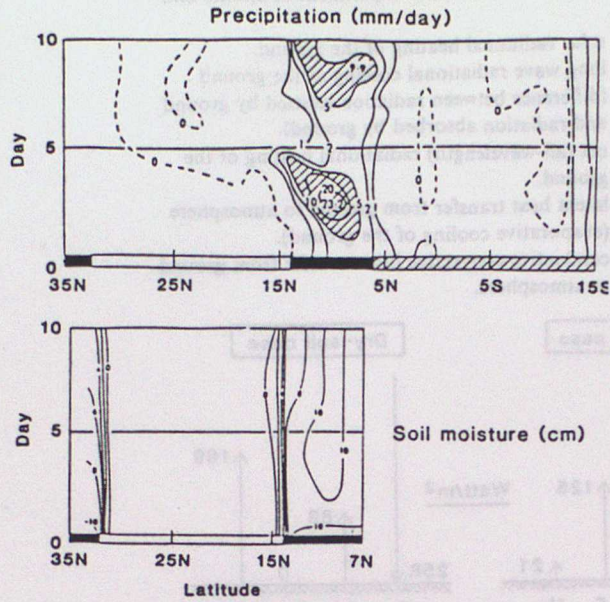


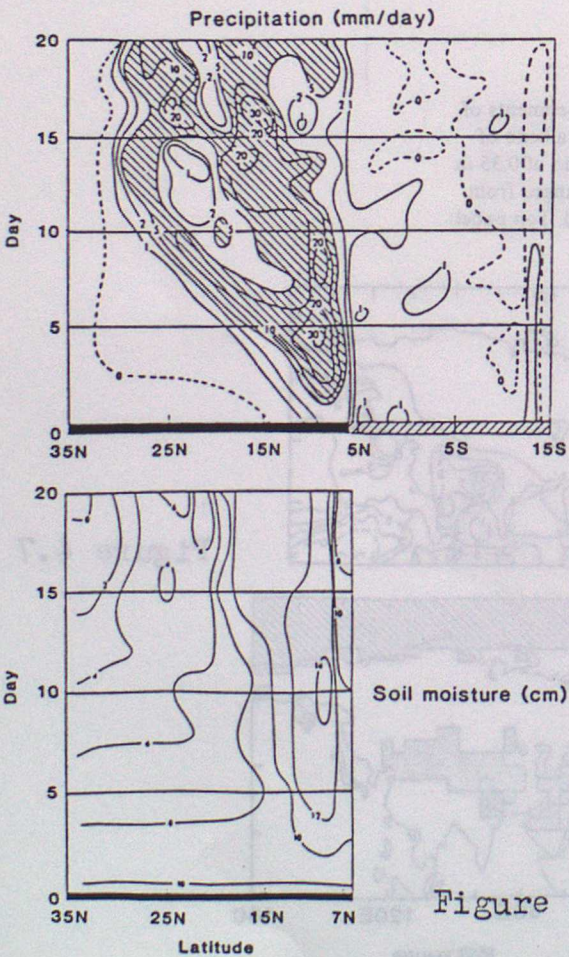
Figure 4.7

The sensitivity of numerically simulated climates

Variation with time of the zonally averaged precipitation (top) and soil moisture (bottom) in the case where, initially, the soil in the Sahara is completely dry. (Experiment of Walker & Rowntree, 1977.)



Variation with time of the zonally averaged precipitation (top) and soil moisture (bottom) in the case where the initial soil moisture in the Sahara is 100 mm. (Experiment of Walker & Rowntree, 1977.)



Variation of the zonally averaged precipitation and soil moisture with time, in selected latitude zones across north Africa, in the case where the initial soil moisture in the Sahara is 100 mm. (Experiment of Walker & Rowntree, 1977.)

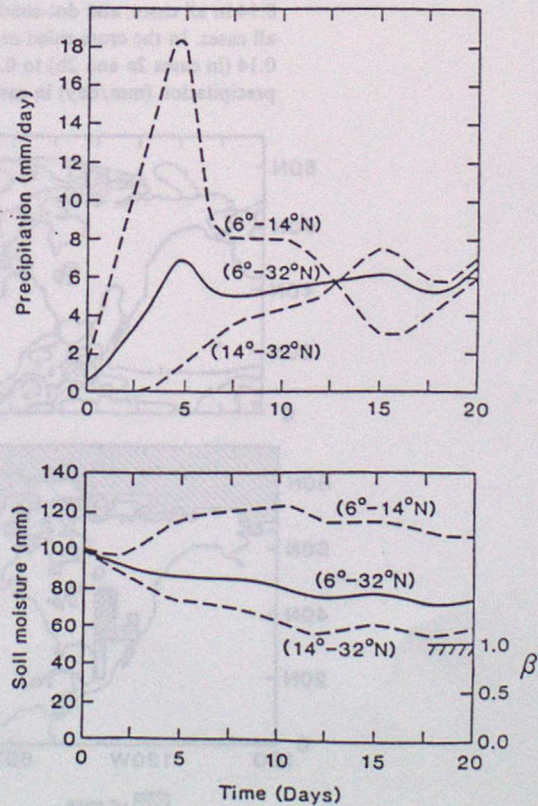


Figure 4.8

.. The world map of annual range of surface temperature.
 (After Monin 1975.)

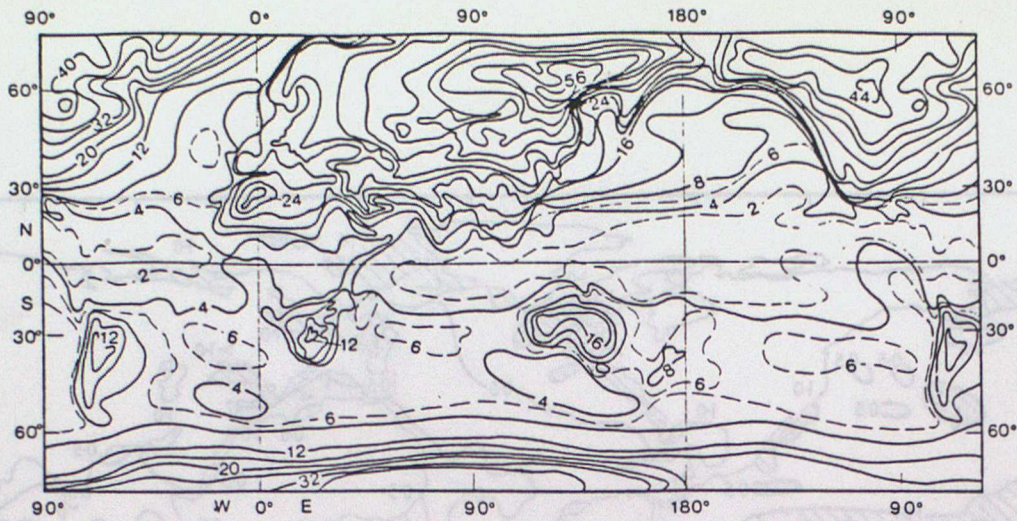
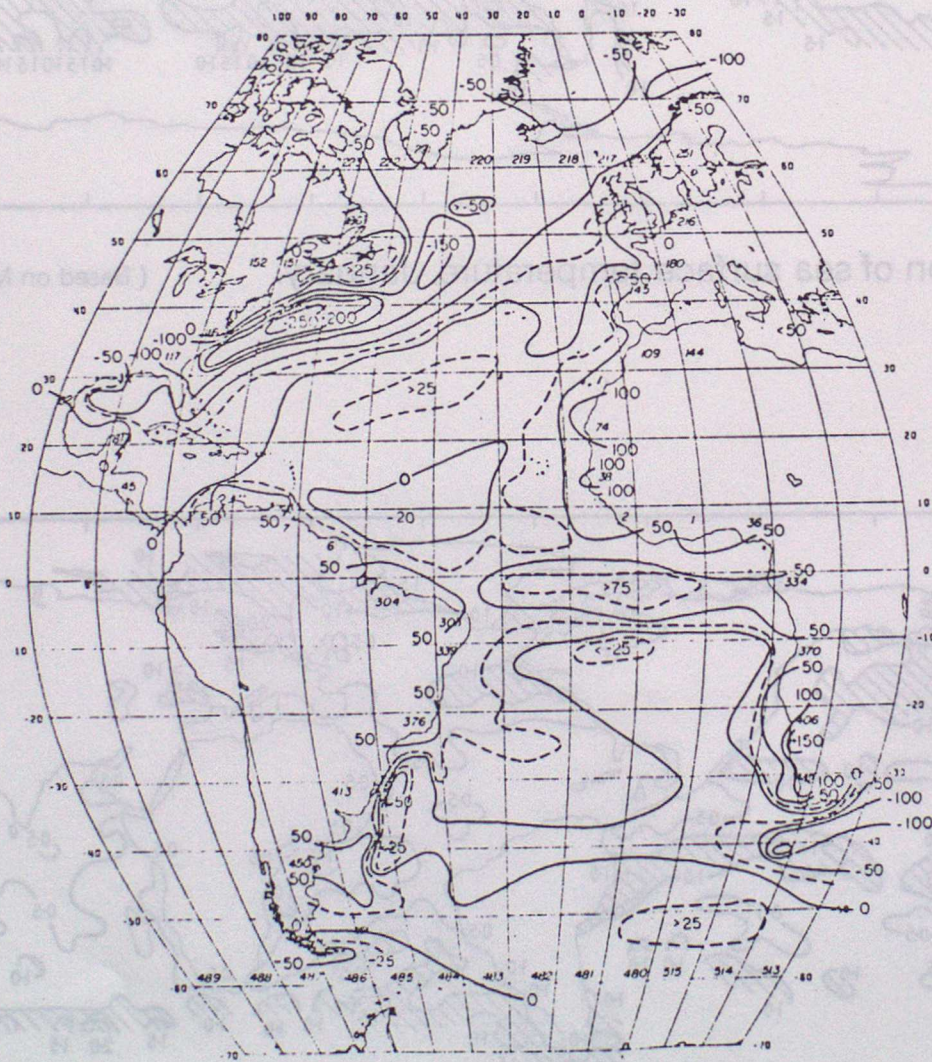


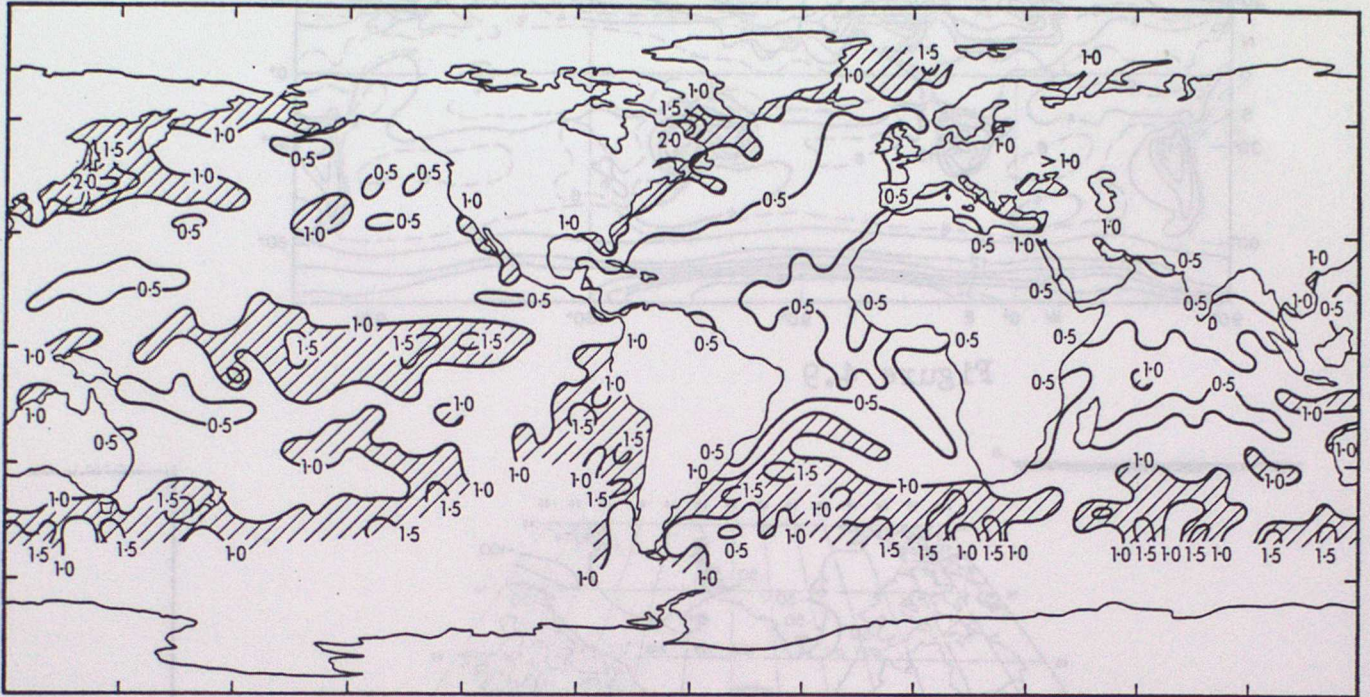
Figure 4.9



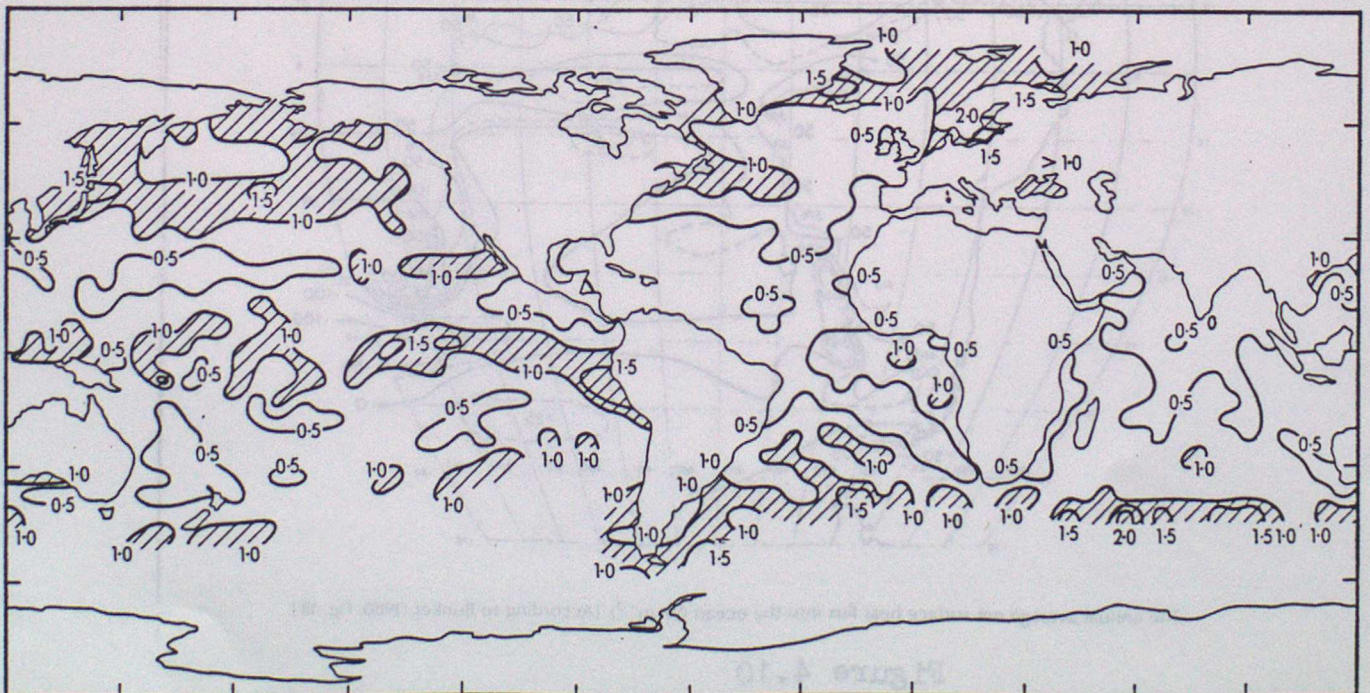
The annual average net surface heat flux into the ocean ($W m^{-2}$). [According to Bunker (1980, Fig. 18').

Figure 4.10

Figure 4.11



Standard deviation of sea surface temperature, January. (Based on MOHSST 3)



Standard deviation of sea surface temperature, July. (Based on MOHSST 3)

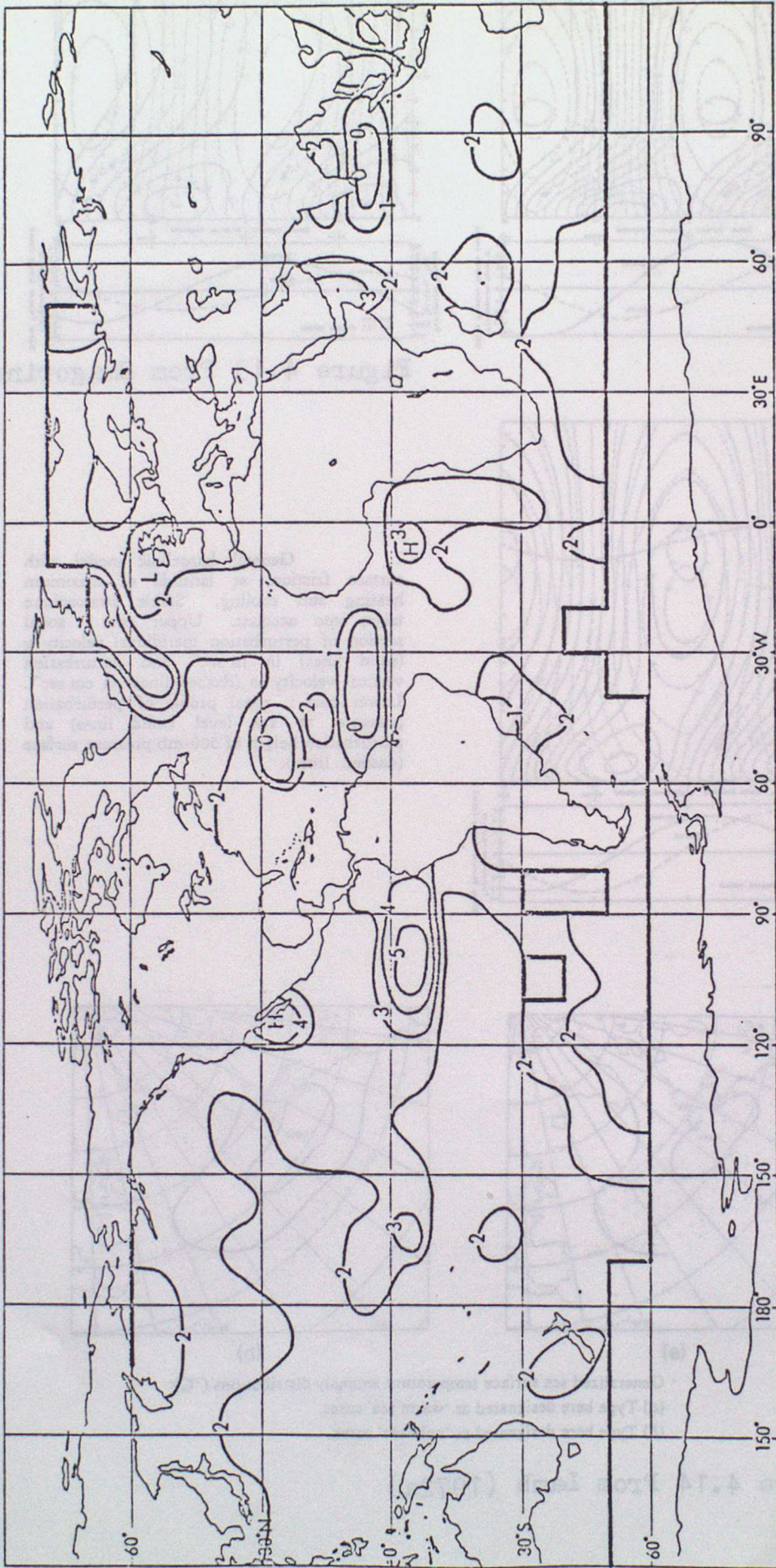


Figure 4.12 Mean lifetime (in months) of a monthly mean $10^\circ \times 10^\circ$ SSTA of magnitude in excess of 1 deg C, based on 1951-1980 data.
 Note: A zero lifetime implies that no 1 deg C anomaly was found in the area between 1951 and 1980.
 From Newman and Storey (1985)

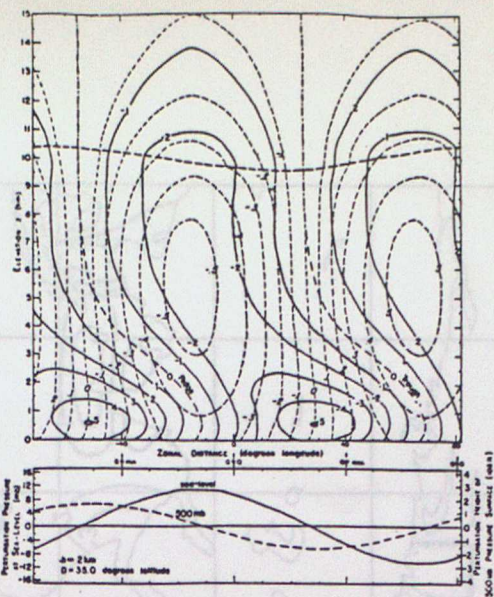
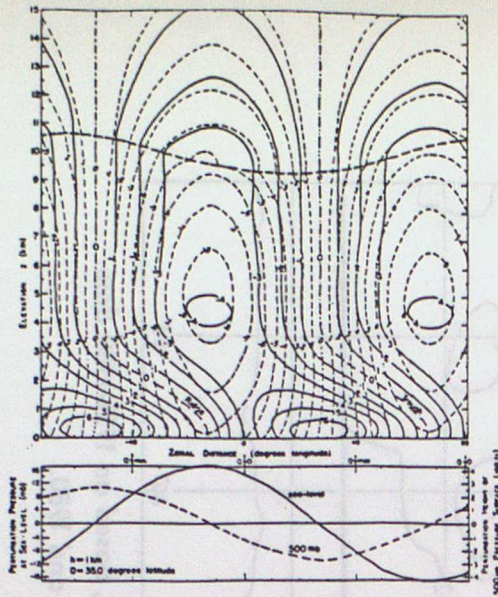
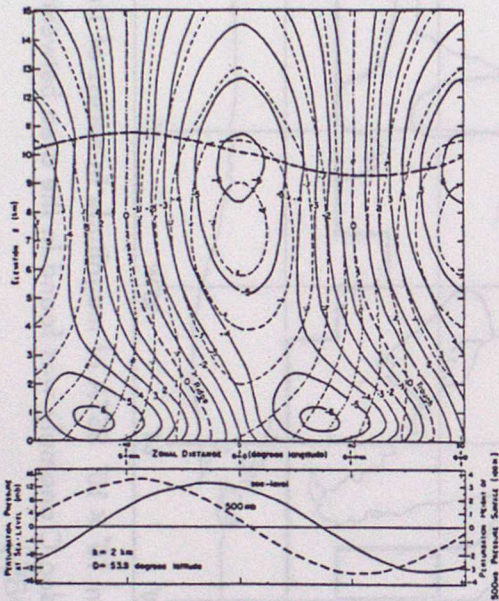
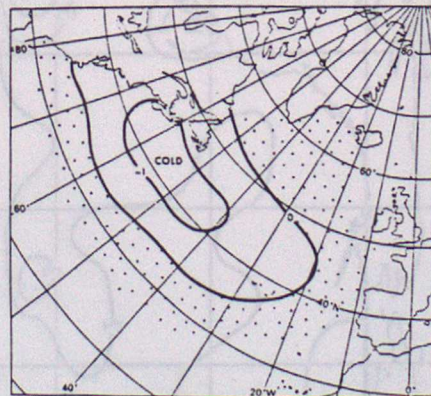
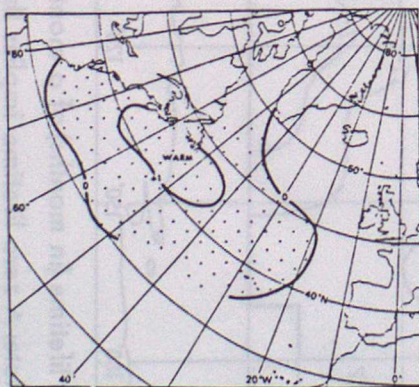


Figure 4.13 From Smagorinsky (1953)



General baroclinic model with surface friction, at latitude of maximum heating and cooling. Stable stratosphere taken into account. Upper part: zonal section of perturbation meridional velocity v (solid lines) in $m\ sec^{-1}$ and perturbation vertical velocity w (dashed lines) in $cm\ sec^{-1}$. Lower part: zonal profile of perturbation pressure at sea level (solid lines) and perturbation height of 500-mb pressure surface (dashed lines).



(a)

(b)

Generalized sea surface temperature anomaly distributions ($^{\circ}C$):
 (a) Type here designated as 'warm sea' cases.
 (b) Type here designated as 'cold sea' cases.

Figure 4.14 From Lamb (1972a)

Figure 4.15a
From Lamb (1972a)

Pressure anomalies (mb) averaged for the following months:
(a) Octobers, given 'warm sea' (fig. 4.14 (a)) in September.
(b) Februarys, given 'warm sea' in January.
(c) Mays, given 'warm sea' in April.
(d) Julys, given 'warm sea' in June.

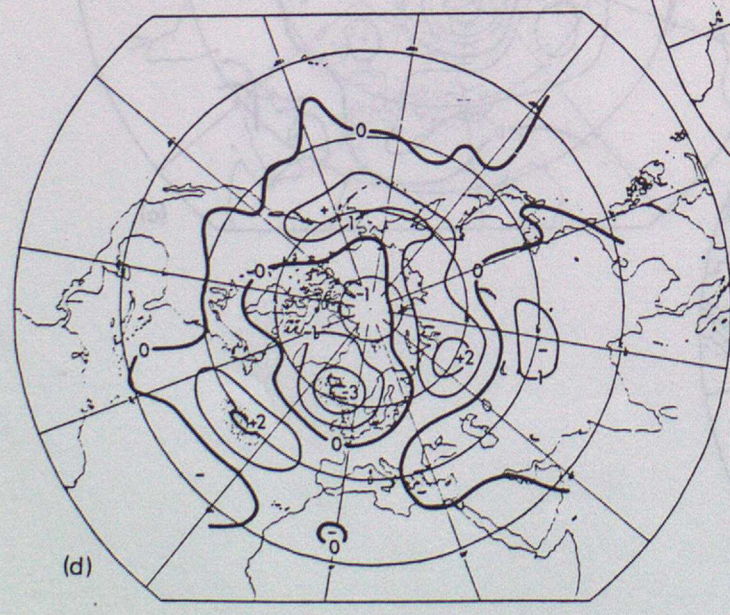
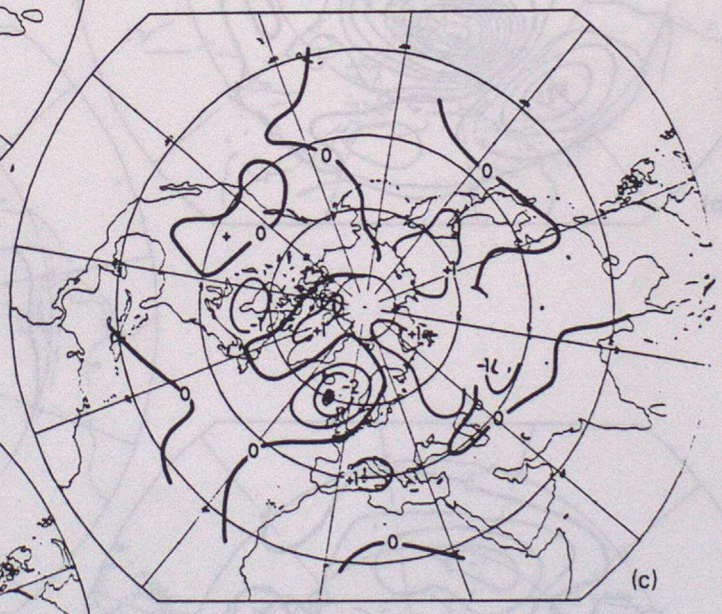
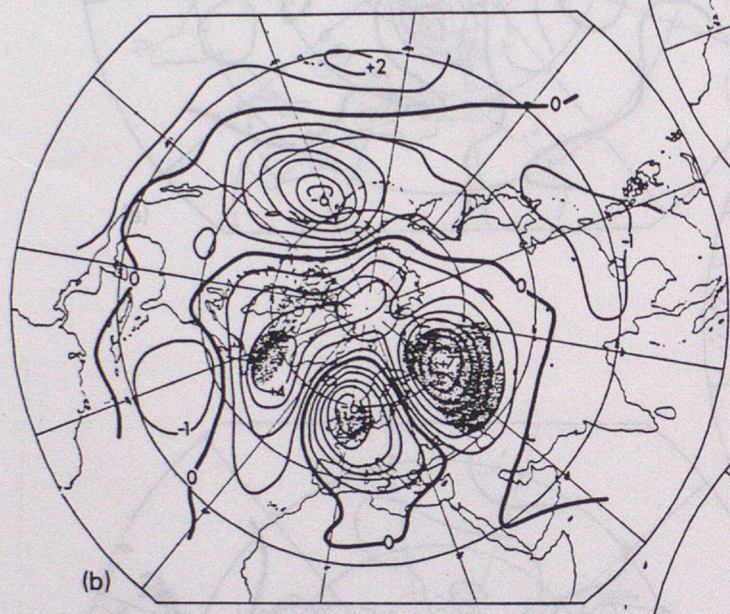
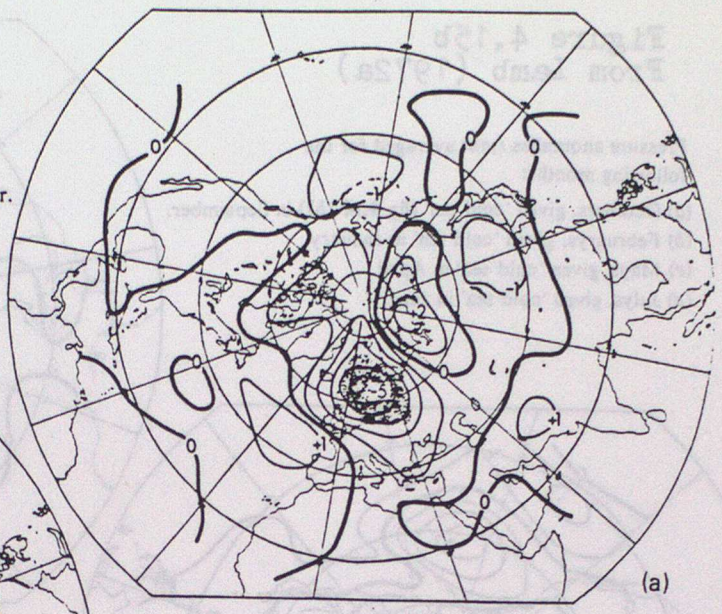
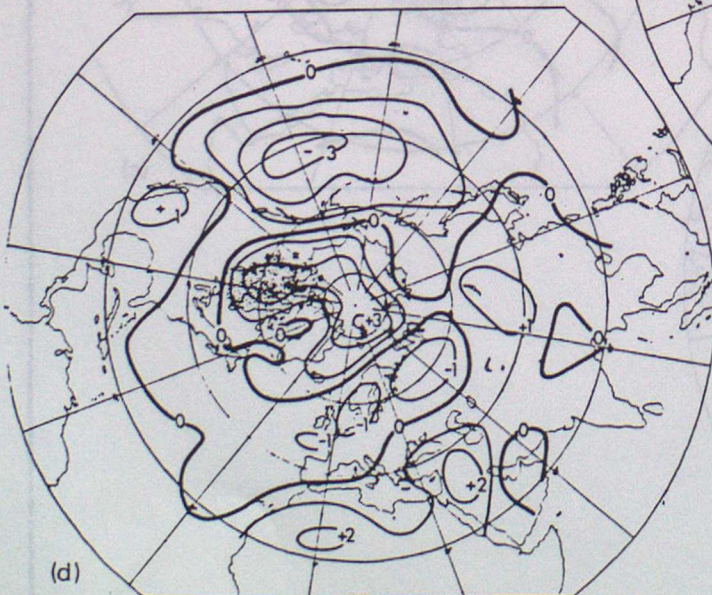
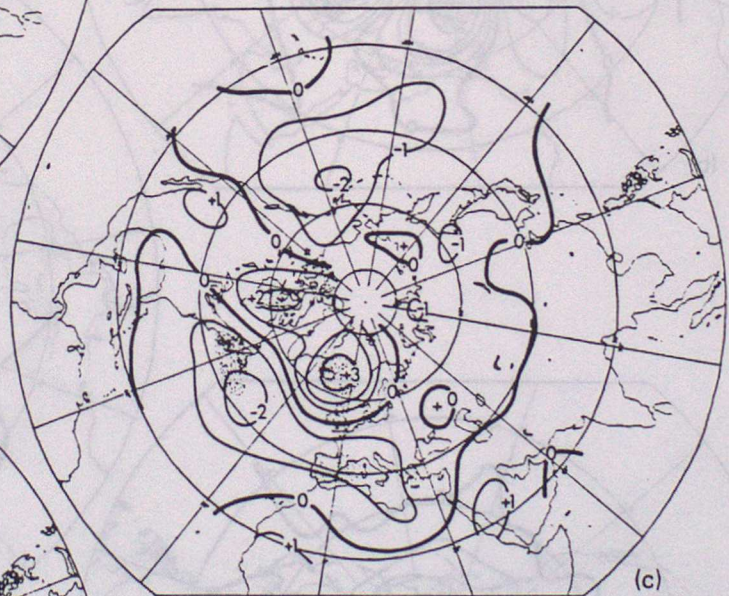
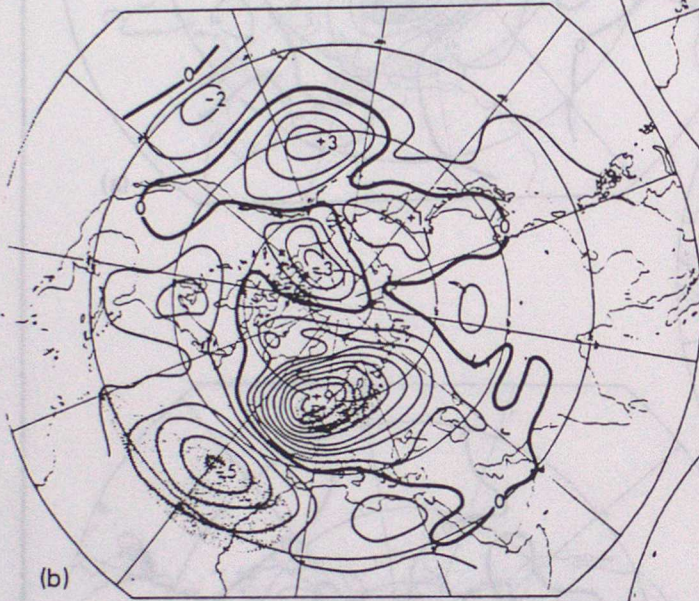
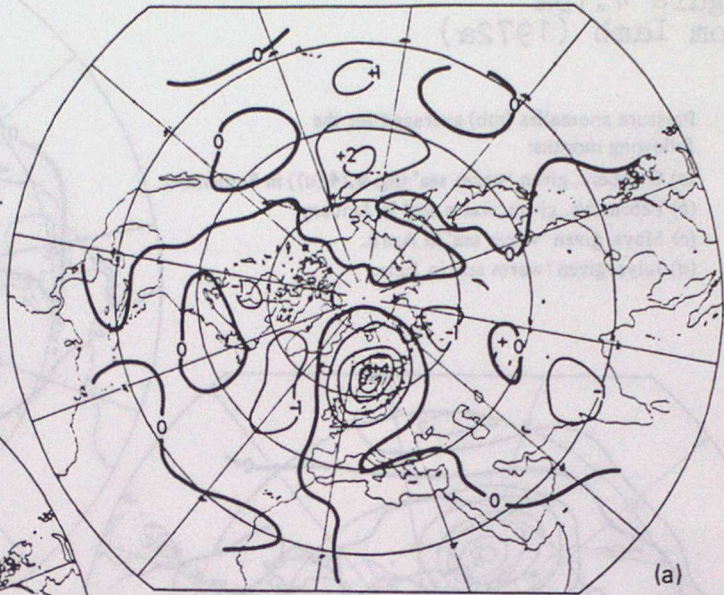
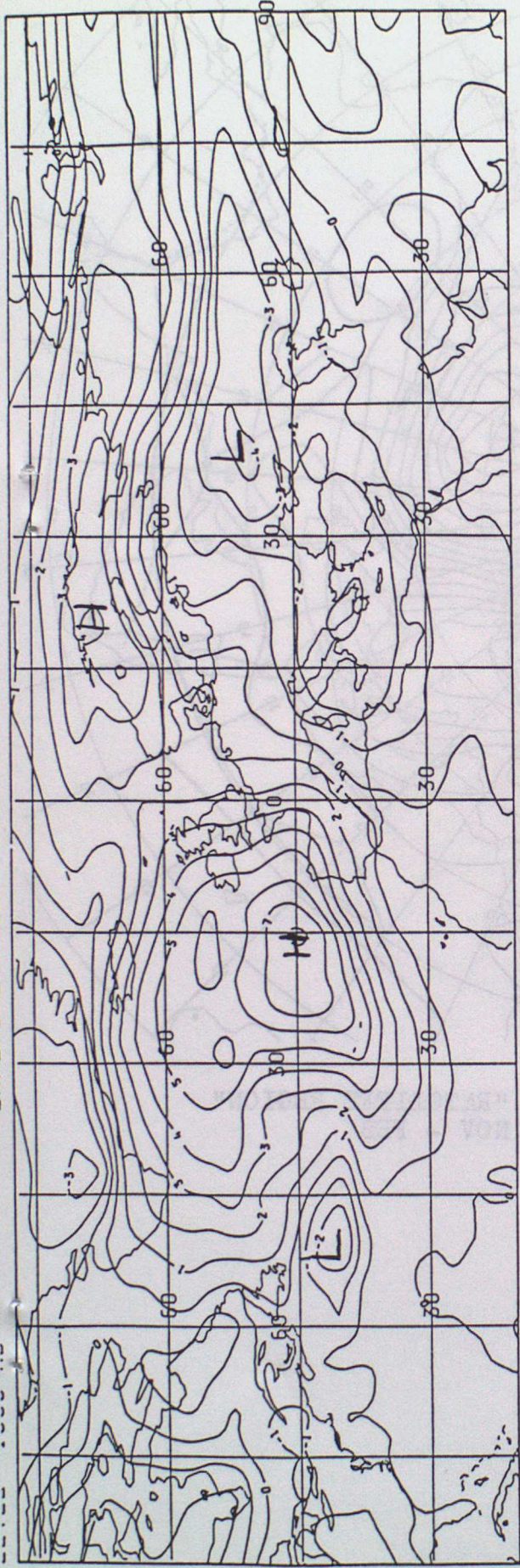


Figure 4.15b
From Lamb (1972a)

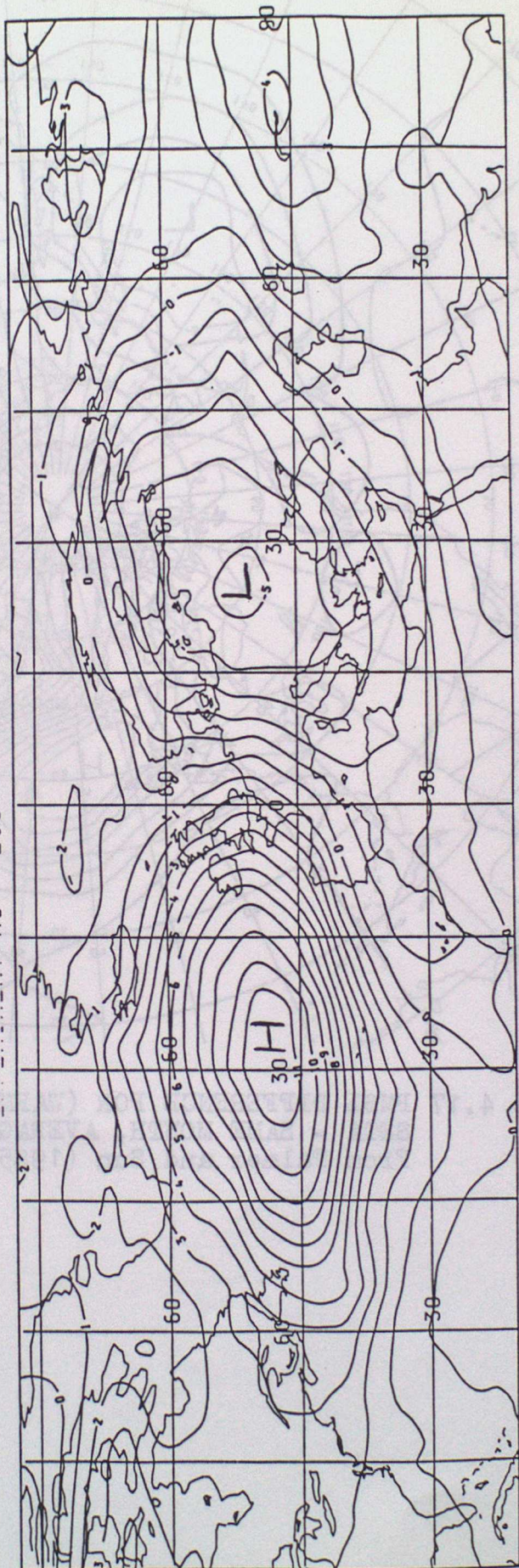
Pressure anomalies (mb) averaged for the following months:

- (a) Octobers, given 'cold sea' (fig. 4.14 (b)) in September.
- (b) Februaries, given 'cold sea' in January.
- (c) Mays, given 'cold sea' in April.
- (d) Julys, given 'cold sea' in June.





A. 1000MB.



B. 500MB.

Figure 4.16 From Palmer and Sun (1985)

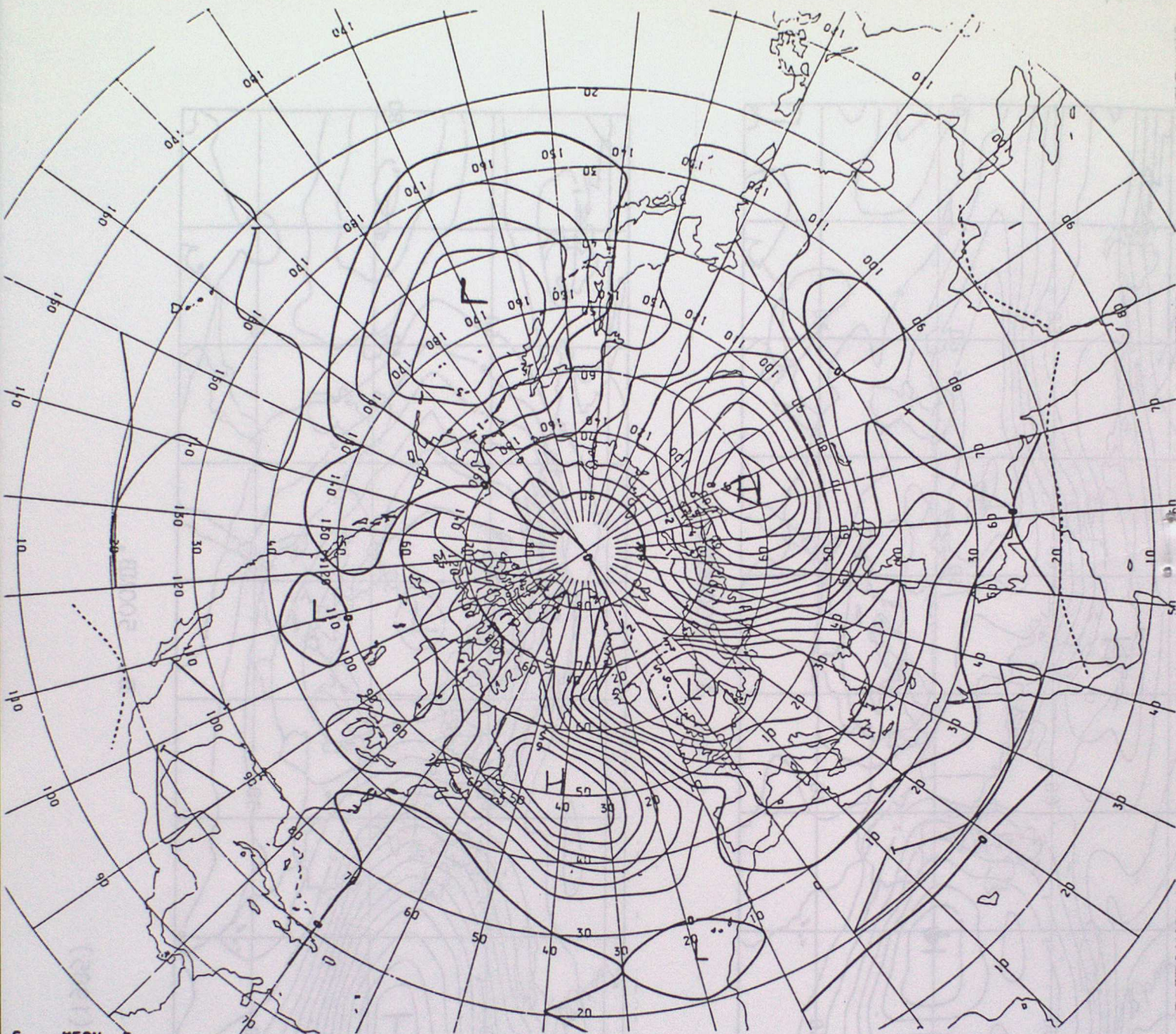


Figure 4.17 PMSL DIFFERENCE FOR (WARM-COLD) "RATCLIFFE REGION"
SSTA - SAME MONTH, AVERAGED FOR NOV - FEB
From Palmer and Sun (1985)

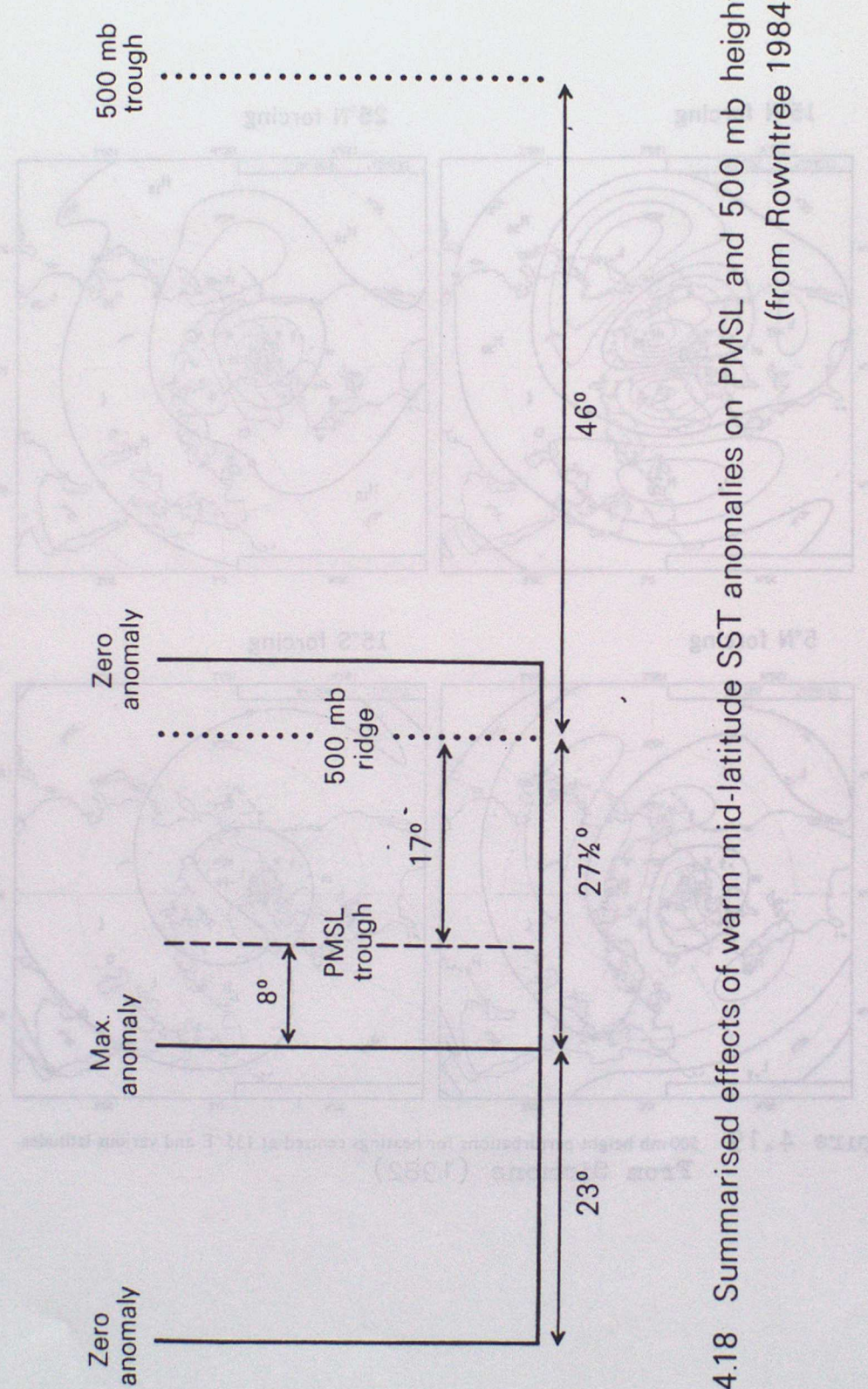


Fig. 4.18 Summarised effects of warm mid-latitude SST anomalies on PMSL and 500 mb height (from Rowntree 1984)

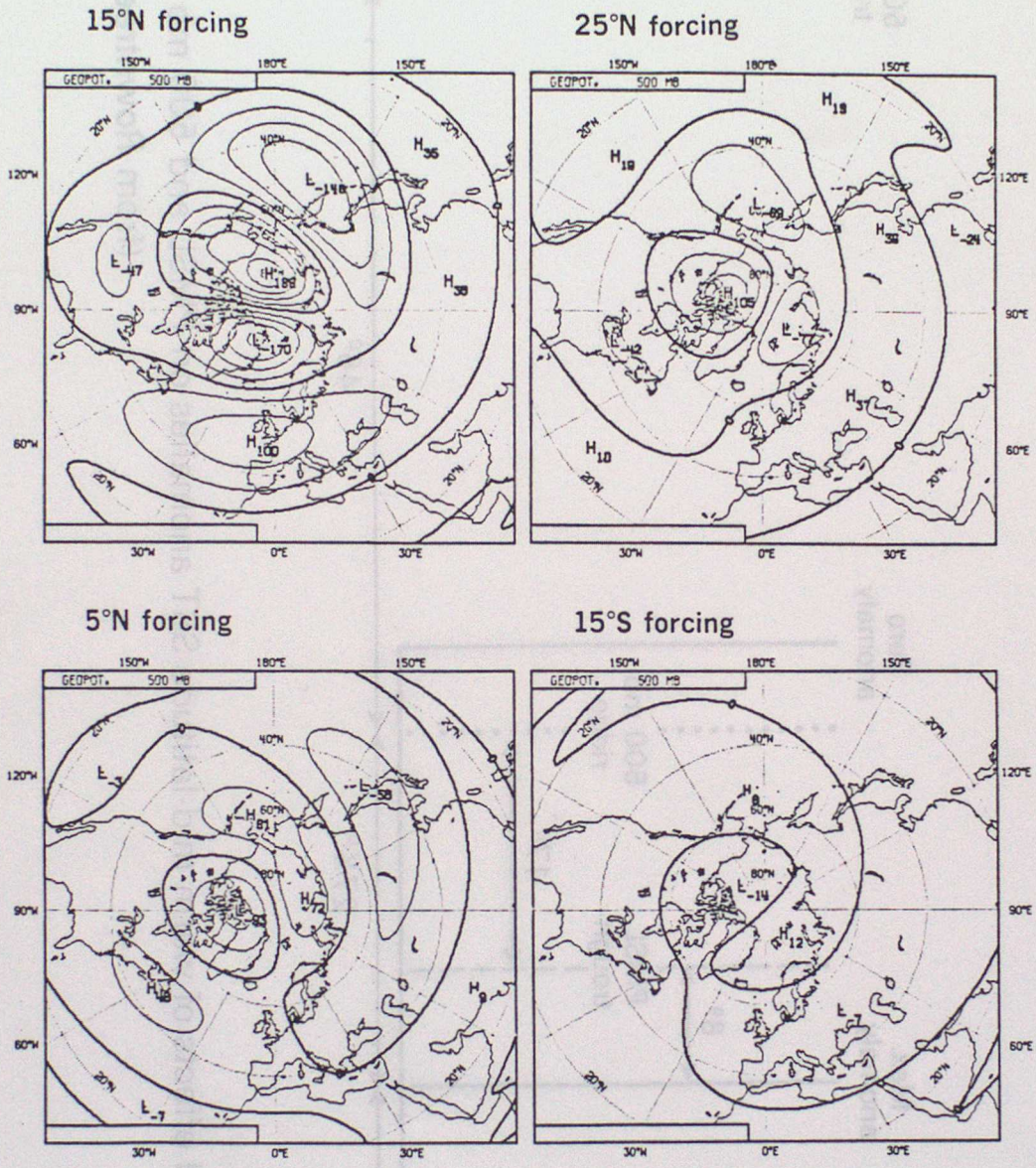
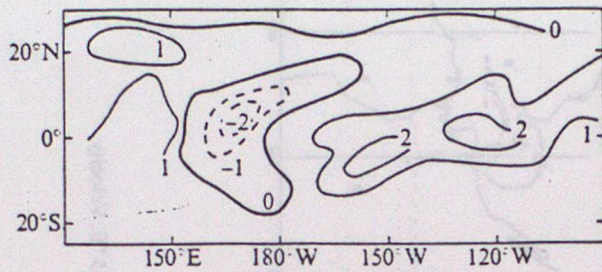


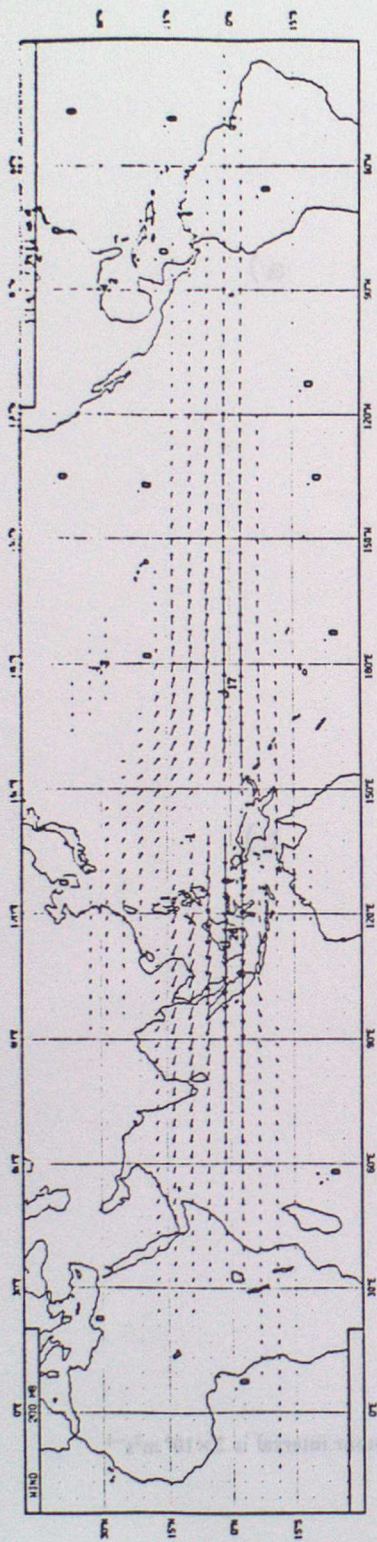
Figure 4.19 500 mb height perturbations for heatings centred at 135°E and various latitudes. From Simmons (1982)



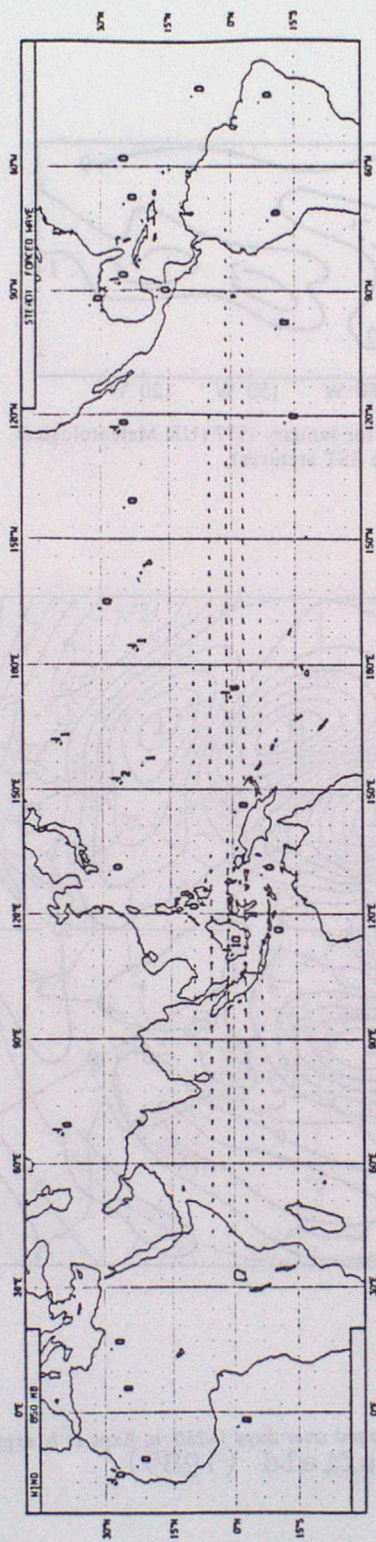
SST anomalies (K) for January 1977 (UK Meteorological Office SST archives).



Figure 4.20 500-mbar streamfunction anomaly averaged over days 1-150. a, Expt 1; b, expt 2. Contour interval is $2 \times 10^6 \text{ m}^2 \text{ s}^{-1}$. From Palmer and Mansfield (1985)



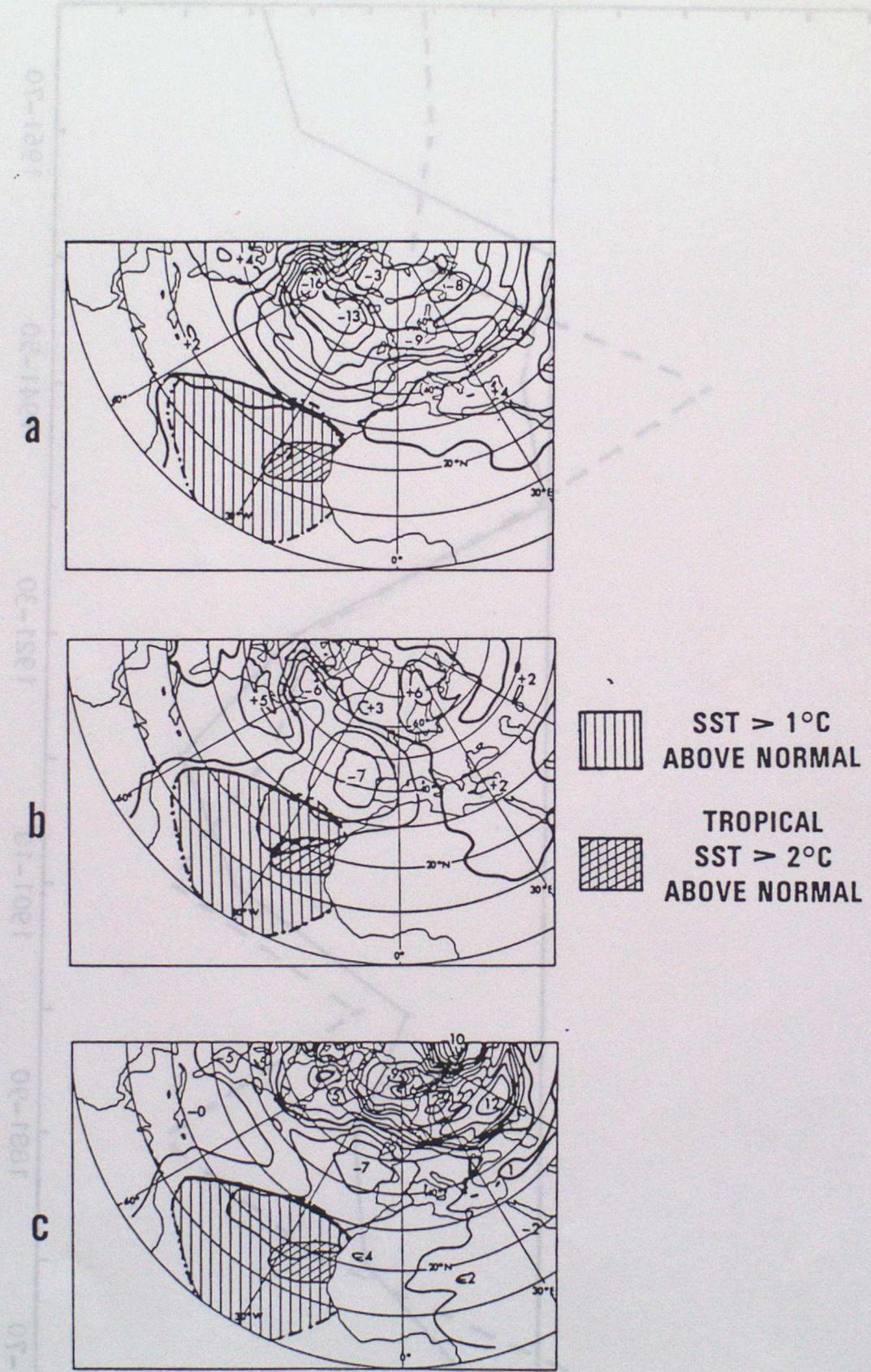
200mb



850mb

Figure 4.21

Perturbation winds at 200 mb and 850 mb for a heating centred on the equator at 135°E. Velocity maxima (in m s^{-1}) are marked. Other details are specified in the text
From Simmons (1982)



Difference in mean surface pressure (mb) averaged over days 41-80 of model integrations between surface pressure obtained with tropical Atlantic warming and the control experiment without the warming. (a) experiment 1 using isothermal initial data, (b) experiment 2 using initial real data, and (c) experiment 3 also using initial real data. Both (b) and (c) use initial data for 29 December 1965. SST averages taken from US Naval Oceanographic Office data.

Figure 4.22 (From Folland (1983))

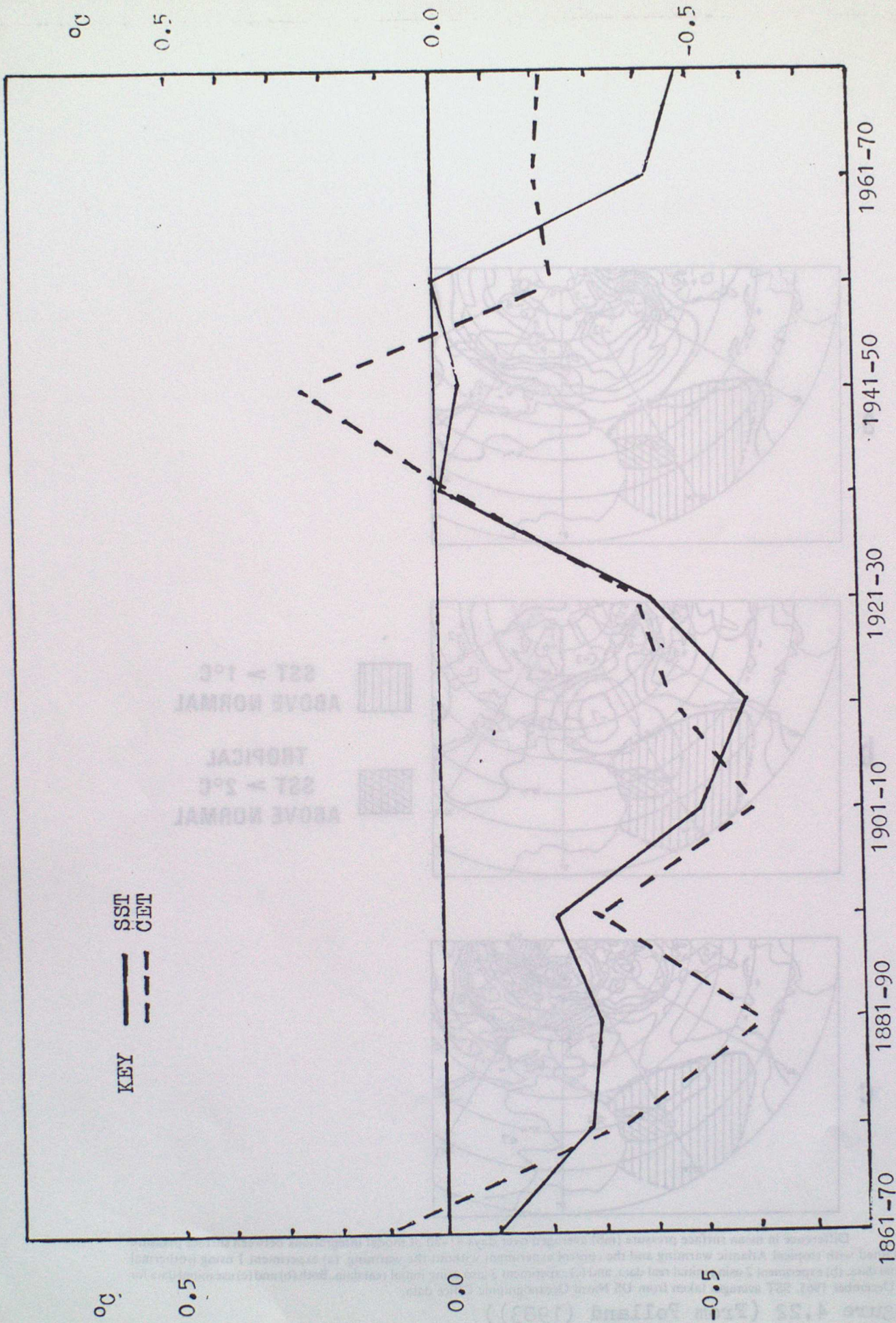


FIGURE 4.23. Decadal anomalies of Central England Temperature (CET) on days with pure 'Westerly' Lamb type, and SST for the Atlantic north of 35°N (with instrumental corrections as in Folland et al (1984)).